



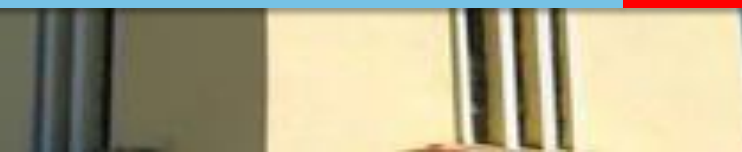
BITS Pilani
Pilani Campus

Presentation

PERFORMANCE BASED SEISMIC DESIGN

NAME(ID): NAMIT SHRIVASTAVA(2020A2PS1767P)

Supervisor : DIPENDU BHUNIA
Department of Civil Engineering

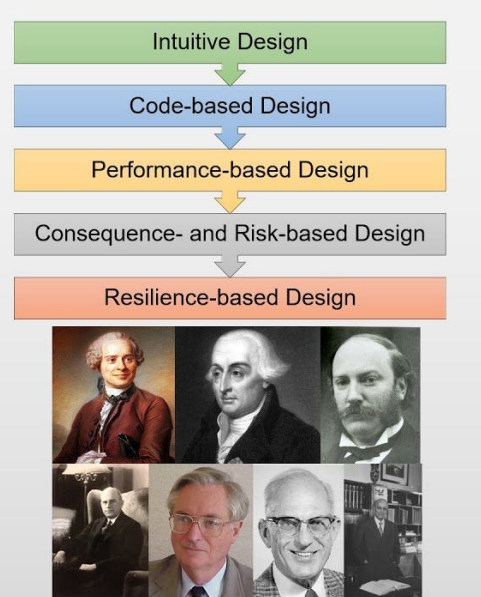


HISTORY

The theory of performance-based seismic design (PBSD) was first proposed in the early 1990s by American scientists and engineers. It piqued the interest of Japanese and European earthquake engineers, who dedicated themselves to it from all angles. The PBSD idea evolved from Moehle's displacement-based seismic design (DBSD) at Berkley University in California. It is based on structural analysis and represents a significant advancement in seismic theory.

PERFORMANCE-BASED SEISMIC DESIGN HISTORICAL BACKGROUND

NONLINEAR MODELLING AND ANALYSIS



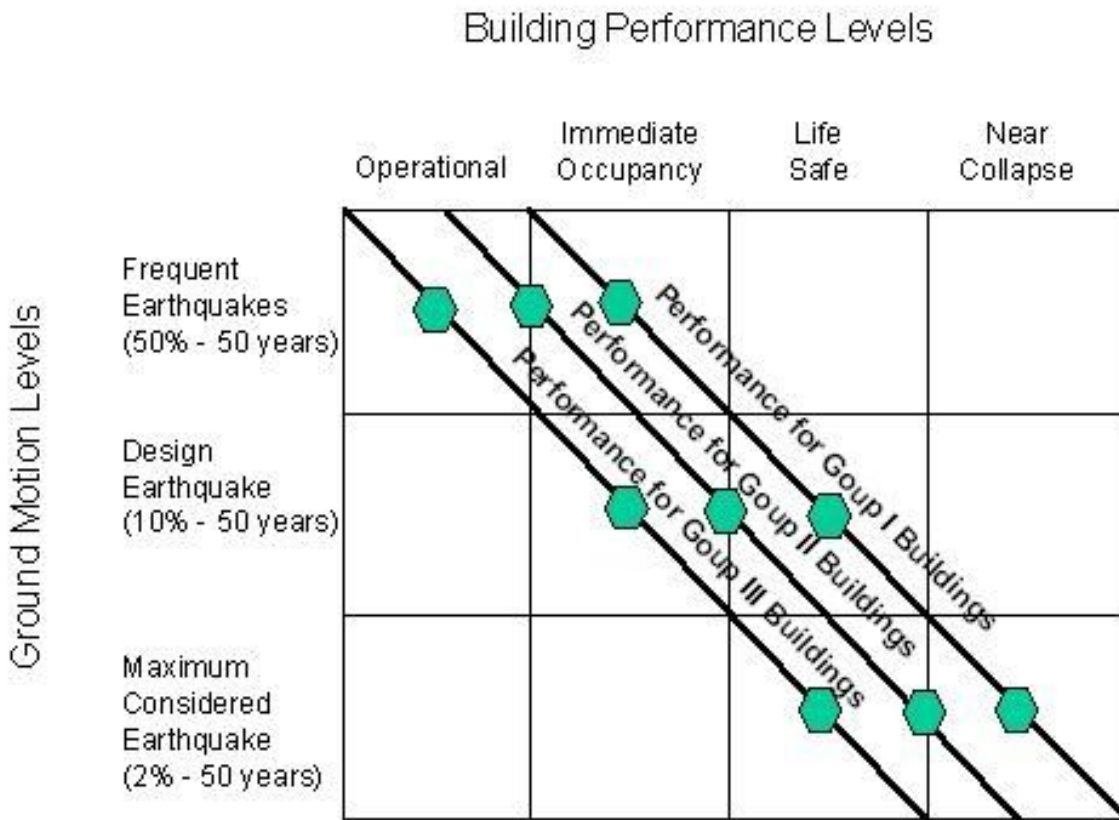
Traditional elastic methods have been used to design structures subjected to seismic loadings. This method arose naturally from the application of elastic analysis methodologies to assess structural performance under working stresses. The ultimate strength provisions have been used to set acceptability standards for load combinations on structures, including seismic effects. Because ductile structures may withstand dynamic loads greater than the elastic limit load, seismic loads are frequently decreased in this process by dividing the loads by ductility factors.

Introduction

- The primary idea behind performance-based seismic design is to give engineers the capacity to design buildings that will behave predictably and consistently in earthquakes.
- As a result, performance-based seismic design is a method for designing new buildings or upgrading existing ones with a realistic awareness of the risk of life, occupancy, and economic damage that future earthquakes may bring.
- The selection of design requirements expressed in the form of one or more performance objectives is the first step in performance-based design. At a given degree of seismic hazard, each performance objective is a statement of the acceptable risk of incurring precise amounts of damage and the resultant losses that occur as a result of this damage.

Distinguishing Characteristics

- Performance Based Seismic Design allows the owner, architect, and structural engineer to choose both the appropriate level of ground shaking and the chosen level of protection for that ground motion.
- Multiple levels of ground shaking can be evaluated, with a different level of performance specified for each level of ground shaking.
- Target building performance levels range from Continued Operation, in which the building and nonstructural components are expected to sustain almost no damage in response to the design earthquake, to Collapse Prevention, in which the structure should remain standing, but is extensively damaged.
- Specific ductility factors ("m" values) are specified for each component of the seismic force-resisting system. The ductility factor varies depending on the target building performance level, material type, and the relative ductility of the component.

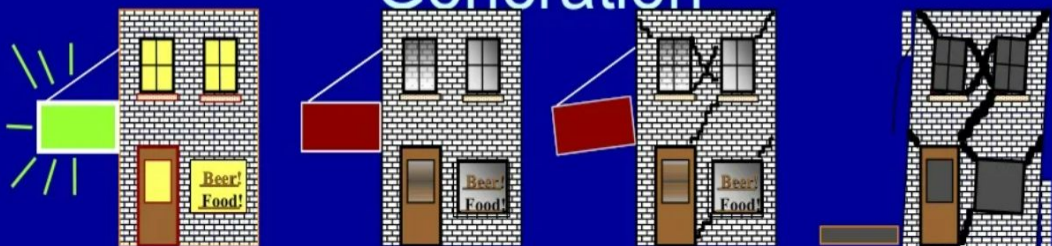


A graphical illustration of a performance objective matrix that compares earthquake hazard levels (y axis) to target building performance levels (x axis) (x axis).

The three diagonal lines show the performance goals for various construction groupings.

Group I is a typical commercial structure, but Groups II and III are structures that require a higher level of security, such as hospitals, fire stations, data centres, critical manufacturing facilities, and so on.

Selecting Performance Present Generation



Operational

*Immediate
Occupancy*

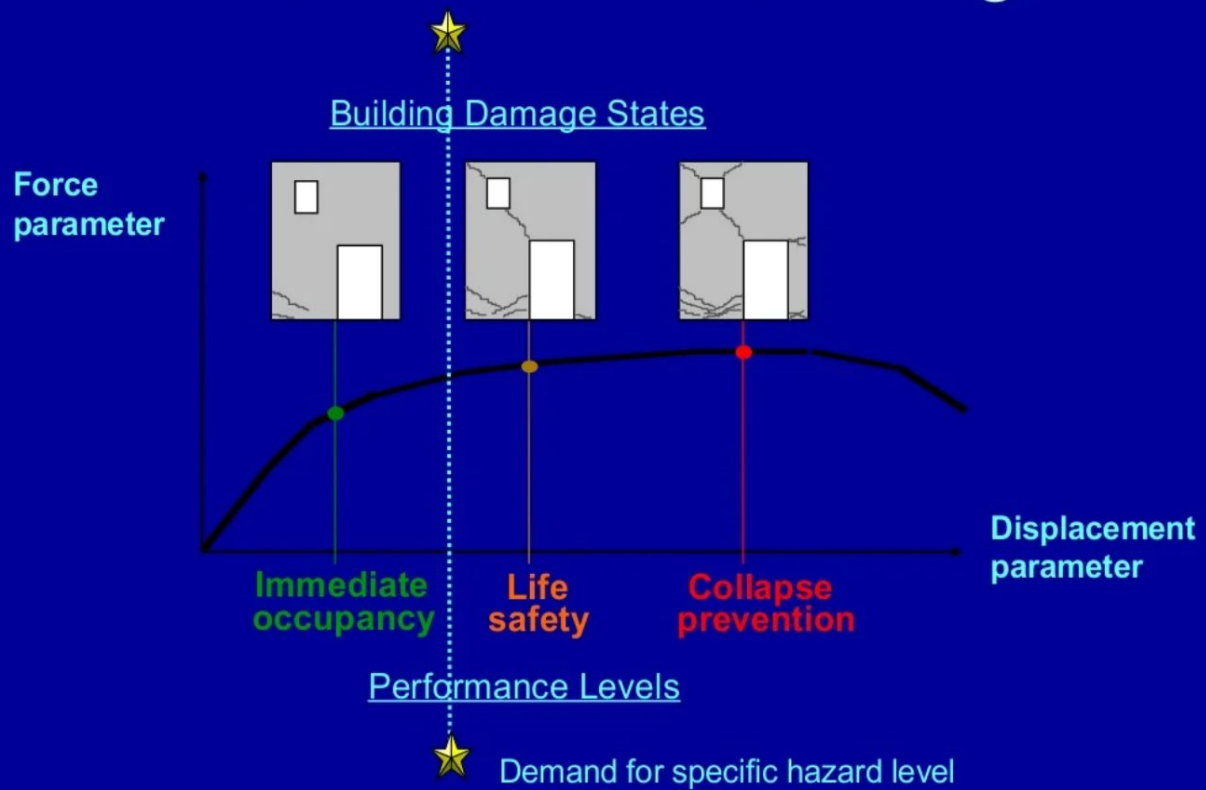
*Life
Safety*

Operational – negligible impact on building

Immediate Occupancy – building is safe to occupy but possibly not useful until cleanup and repair has occurred

Life Safe – building is safe during event but possibly not afterward

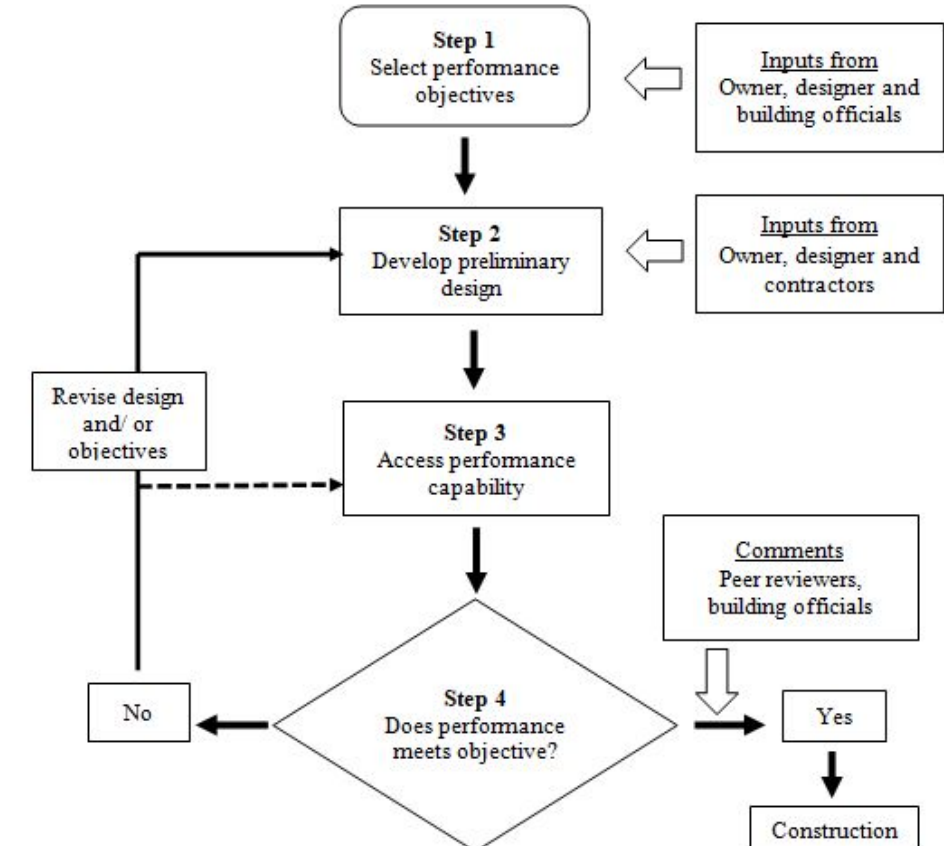
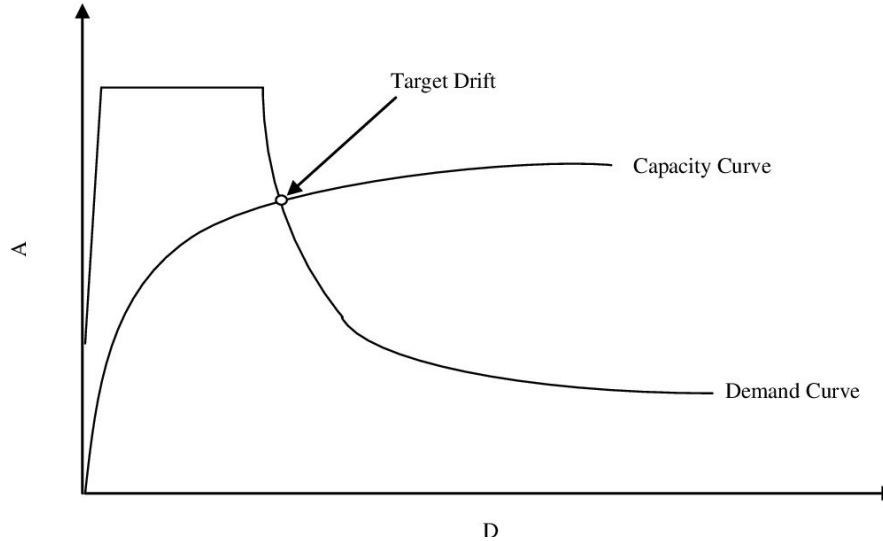
Performance based design



Design methods used by PBSD theory

A set of rational function levels is established, and quantitative metrics such as beam and column bending, shear, and axial deformation, as well as plastic performance of their connections, are given.

The target performances are decided by the structure's role and importance. The distinction between the PBSD seismic design approach and the typical structural design system is the emphasis on displacement properties and nonlinear inelastic static analysis of structures.



Displacement Influence Factor Method

The method is used to determine the maximum expectation displacement in structure static analysis. The displacement is defined as target displacement δ_t :

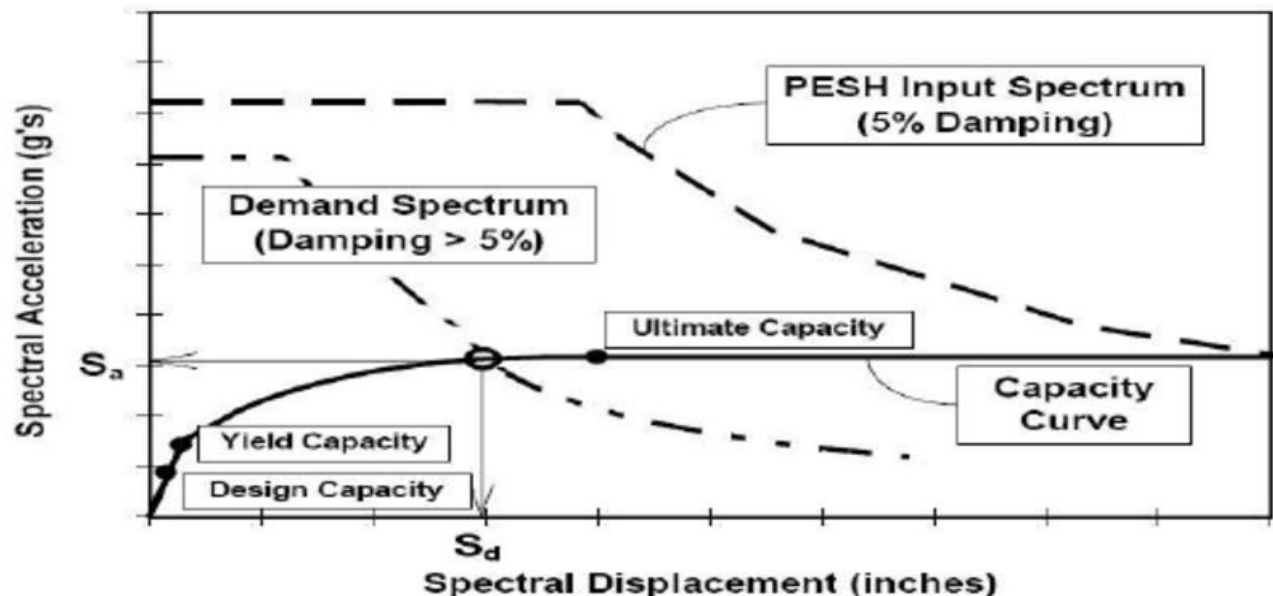
$$\delta_t = c_0 c_1 c_2 c_3 s_a \frac{T_e}{4\pi^2} G$$

here, c_0 is the ratio of displacement of equivalent SDOF system to roof displacement of structure; c_1 is the ratio of the maximum nonlinear expectation displacement to linear displacement; c_2 is an influence factor to the maximum displacement response by shape of hysteretic hoops; c_3 is an influence factor by P-Δ effect; s_a is spectrum response acceleration with real nature period and damp, and T_e is the nature period of structure.

The key point of the method is to simplify the MDOF system into SDOF system, but further study of abstraction method and accuracy is needed, this method is only used to predict the whole performance, and the performance of structure elements cannot be embodied.

Capacity Spectrum Method

Capacity spectra are obtained by pushover analysis. In the pushover analysis the six equations of motion are used to obtain the column forces due to incremental lateral forces at the mass centre. As the equations of motion contain the contribution due to eccentricities the column forces do exhibit the influence of rotations about the vertical axis. Plots of spectral acceleration Vs spectral displacement (ADRS format) are obtained from independent spectral acceleration and spectral displacement spectra for various levels of ductilities. Juxtaposing one on the other will confirm the ductility required for the given yield acceleration.



FORESEE RESEARCH AND APPLICATION



The theory of PBSD is not mature yet. Further researches are needed before it is used extensively.

- To the earthquake risk, transition from intensity to zonation according to ground motion parameters is required. The meanings of minor, moderate and major earthquake should be defined clearly. In China, the new mapping is finished on the basis of earthquake action factor $K = \alpha g$ and characteristic period T_g .
- To the structure performance, the obscure meanings of non-damage, repairable and no collapse and so on should be verified. The target performance levels should be defined quantitatively.
- To the response spectrum used in design, long period component, near-field effect and duration of earthquake should attract attention, and velocity spectrum, displacement spectrum, energy spectrum and/or capacity spectrum may substitute the acceleration spectrum in design.
- To the design method, the linearity method of transmitting from MDOF to equivalent SDOF system should be improved or completed to make PBSD applicable.
- To the standard of damage and function destroyed, the probability norm may be more suitable, and the subentry factor method used to describe limit state may be modified.

Classification of districts of Rajasthan according to seismic zones:

S. No.	Seismic Zone	Intensity (MSK)	Magnitude	Districts
1	IV [High Damage Risk Zone]	VII-VIII	6.0 – 6.9	Some parts of Barmer [Chohtan Block], Jalore [Sanchore Block] Alwar [Tijara Block], and Bharatpur [Block Nagar, Pahari]
2	III [Moderate Damage Risk Zone]	VI-VII	5.0 – 5.9	Some parts of Udaipur , Dungarpur , Sirohi , Barmer , Jaisalmer , Bikaner , Jhunjhunu , Parts of Sikar, Jaipur, Dausa, and Bharatpur.
3	II [Low damage Risk Zone]	IV-VI	4.0 – 4.0	Ganganagar, Hanumangarh, Churu, Jodhpur, Pali, Rajasamand, Chittorgarh, Jhalawar, Baran, Kota, Bundi, Sawai Madhopur, Karauli, Dholpur, Banswara, some areas of Bikaner, Udaipur, Jhunjhunu, Sikar, and Jaipur.

Seismic Faults in Rajasthan

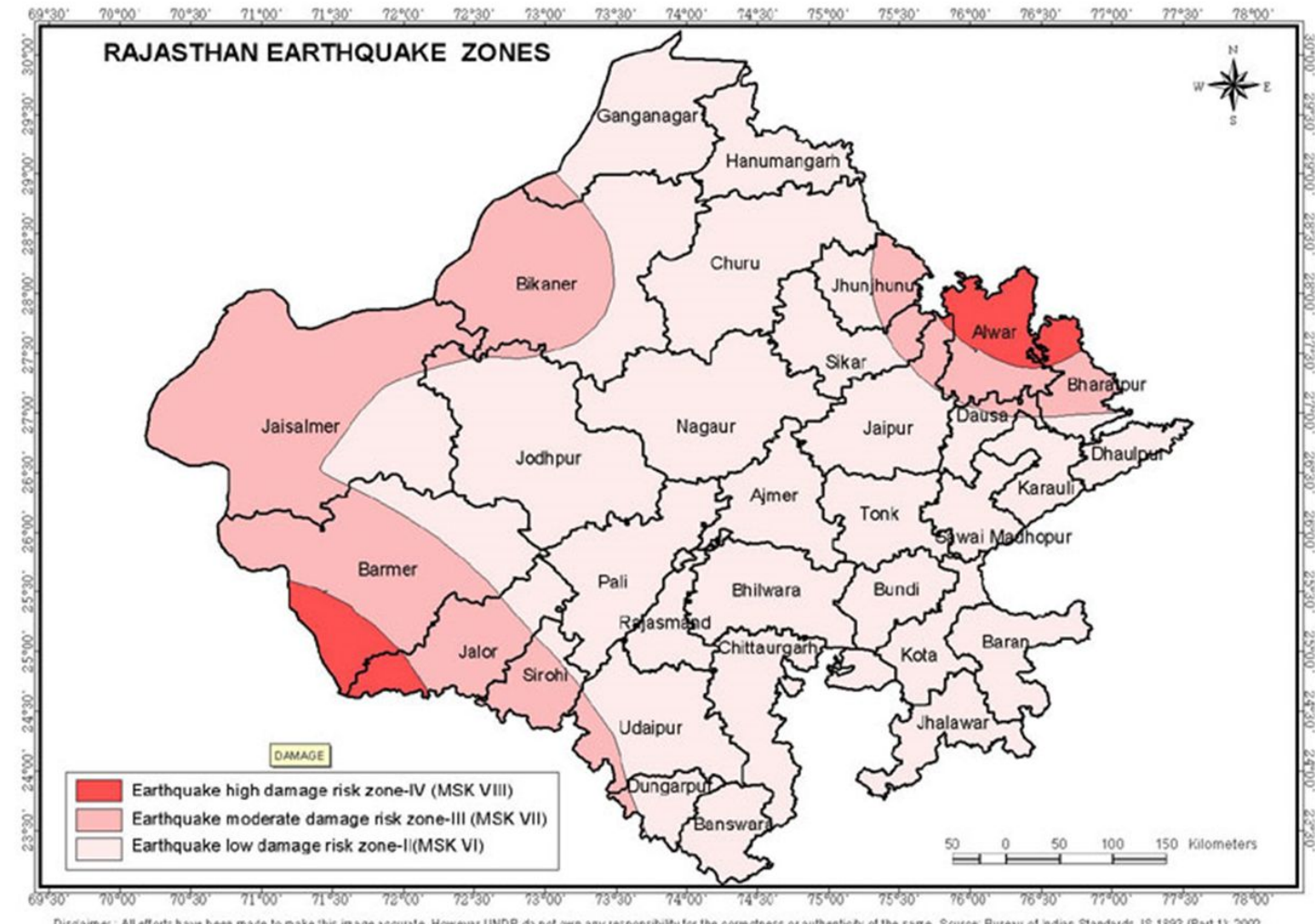
Several faults have been identified in [Rajasthan](#), out of which many show evidence of movement during the Holocene epoch.

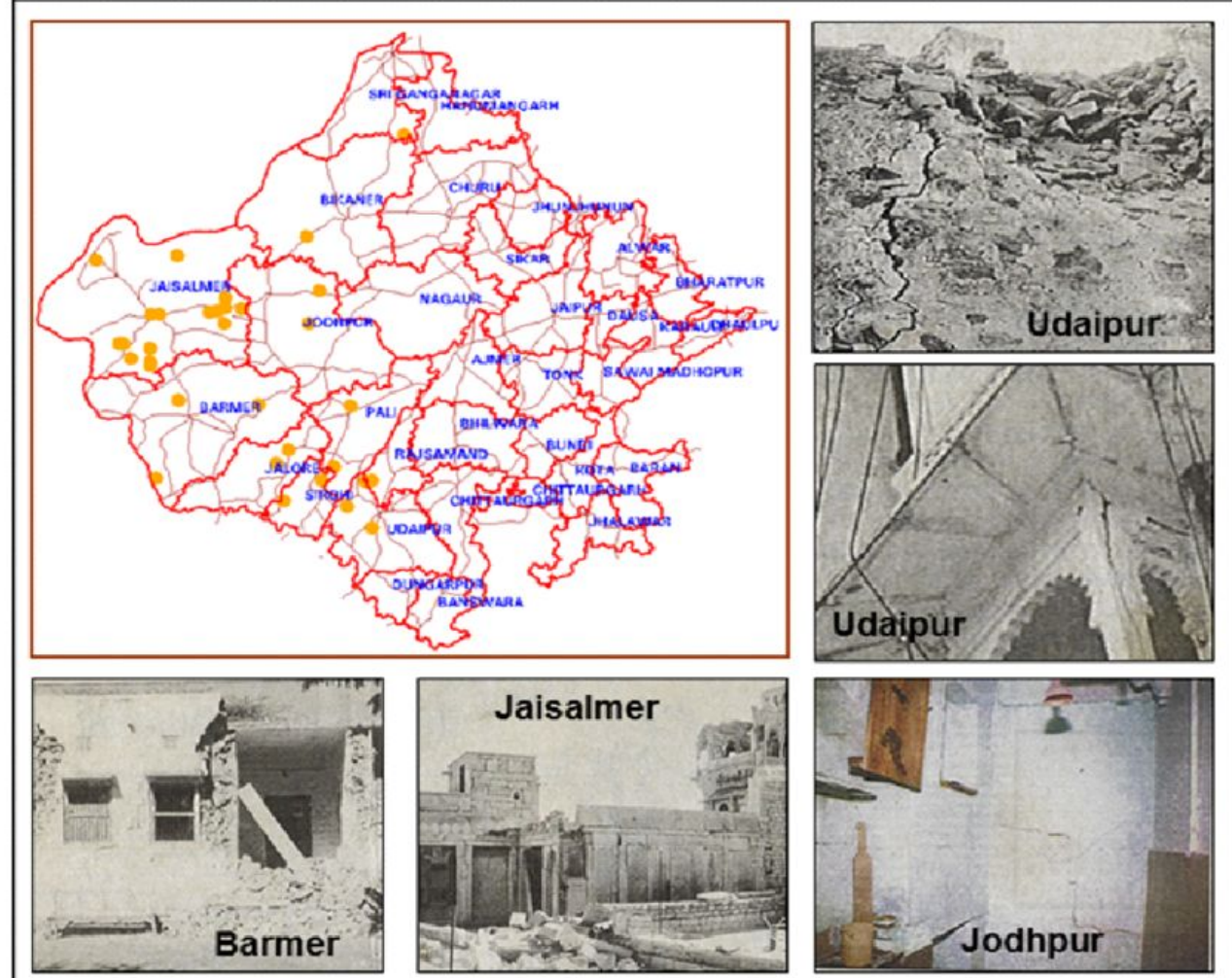
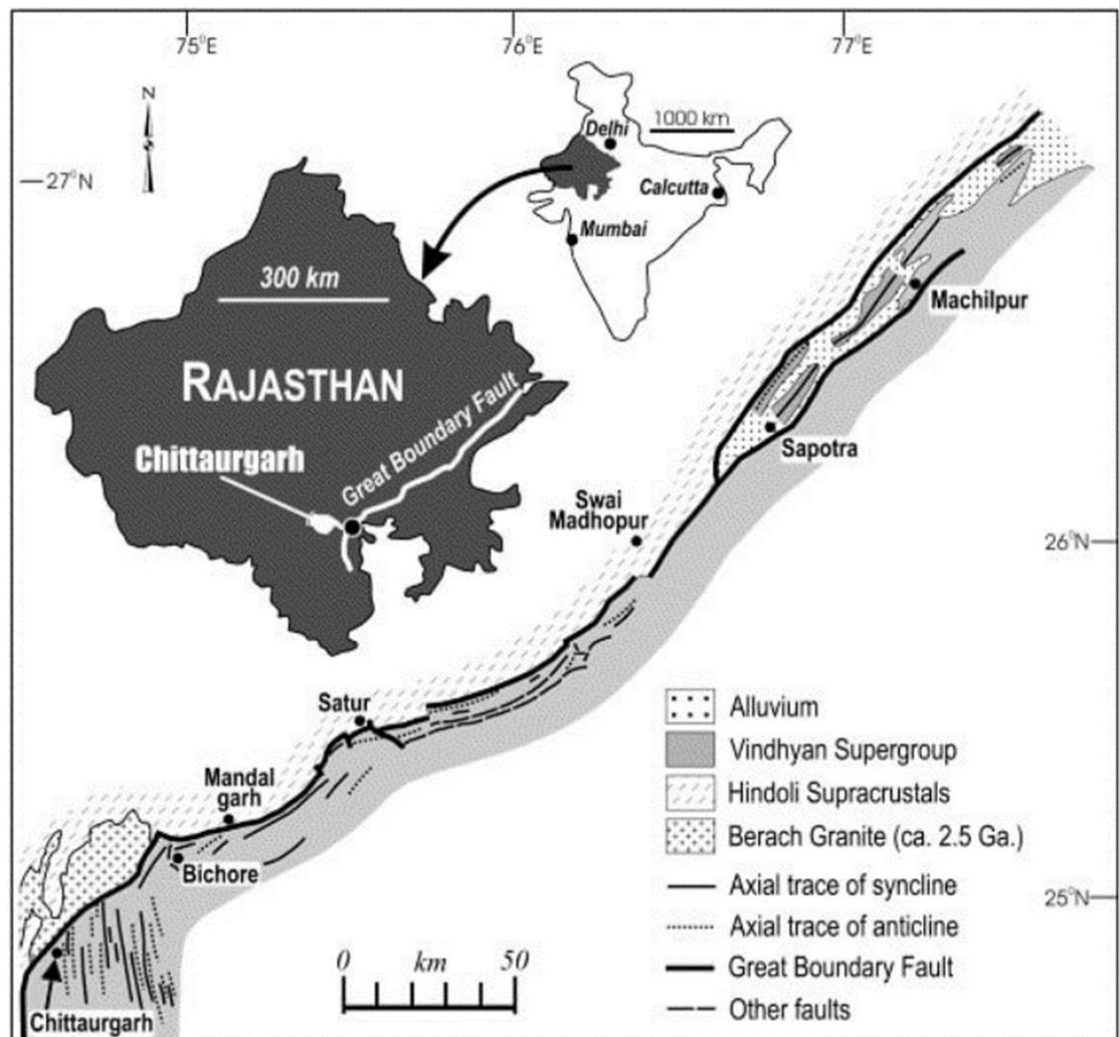
- The **Cambay Graben** terminates in the south-western part of the state.
- The **Konoi Fault** near [Jaisalmer](#) trends in a north-south direction and was associated with the 1991 Jaisalmer earthquake.

Several active faults criss-cross the Aravalli range and lie parallel to each other.

- The most prominent of them is the north-south trending **Sardar Shahar Fault** and
- The **Great Boundary Fault** which runs along the [Chambal River](#) and then continues in the same direction into Uttar Pradesh.

Medvedev–Sponheuer–Karnik scale, also known as the MSK or MSK-64, is a macroseismic intensity scale used to evaluate the severity of ground shaking on the basis of observed effects in an area where an earthquake transpires

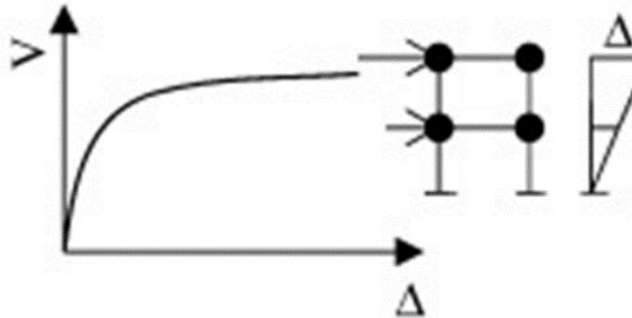
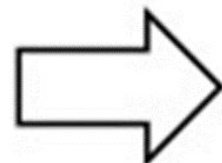




Required Capacity of Nonlinear Deformations of the SDOF System with the Pushover Analysis

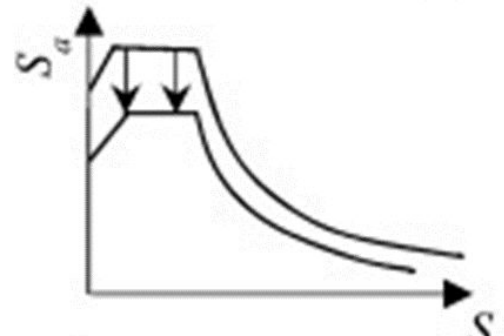
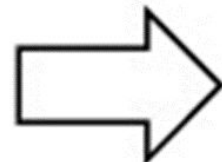
Obtaining capacity spectrum

Represents the lateral displacement as a function of force applied to the structure in ADRS format



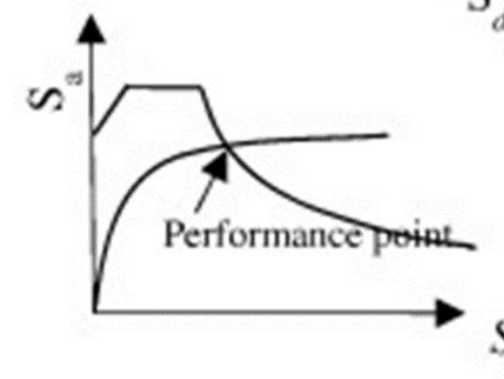
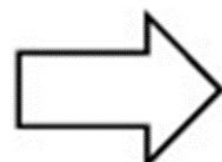
Obtaining demand Spectrum

For a given structure and ground motion, displacement demand is estimated for maximum expected response of



Obtaining performance point

Intersection point of demand spectrum and capacity spectrum



Pushover analysis is a static process that estimates seismic structural deformations using a reduced nonlinear technique.

During earthquakes, structures remodel themselves. The dynamic forces on a structure are moved to other components as individual components yield or fail.

The design eccentricity is a function of the structural eccentricity, which is defined as the distance between the center of rigidity at a level and the resultant of all lateral forces at that level.

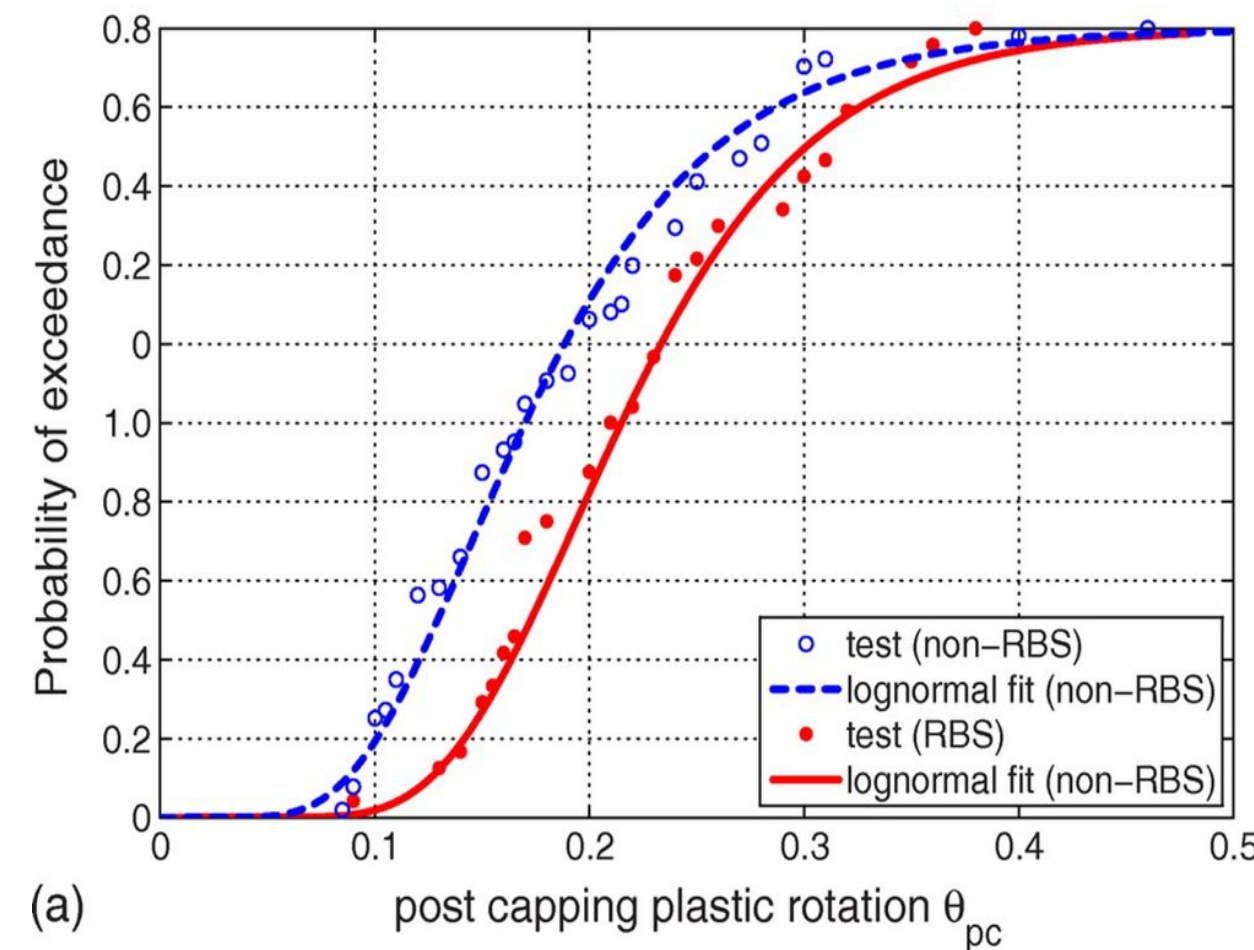


	T _R =2475yr			T _R =975yr			T _R =975yr <i>classical hazard, equal in all cases</i>
	<u>SITE A</u>		<u>SITE B</u>	<u>SITE A</u>		<u>SITE B</u>	
	G-R	CE	G-R	G-R	CE	G-R	
S _a (T=0.50s)	0.612 g	0.466 g	0.456 g	0.418 g	0.296 g	0.309 g	0.293 g
S _a (T=0.75s)	0.458 g	0.382 g	0.352 g	0.294 g	0.221 g	0.229 g	0.215 g
S _a (T=1.00s)	0.348 g	0.303 g	0.271 g	0.213 g	0.167 g	0.172 g	0.161 g

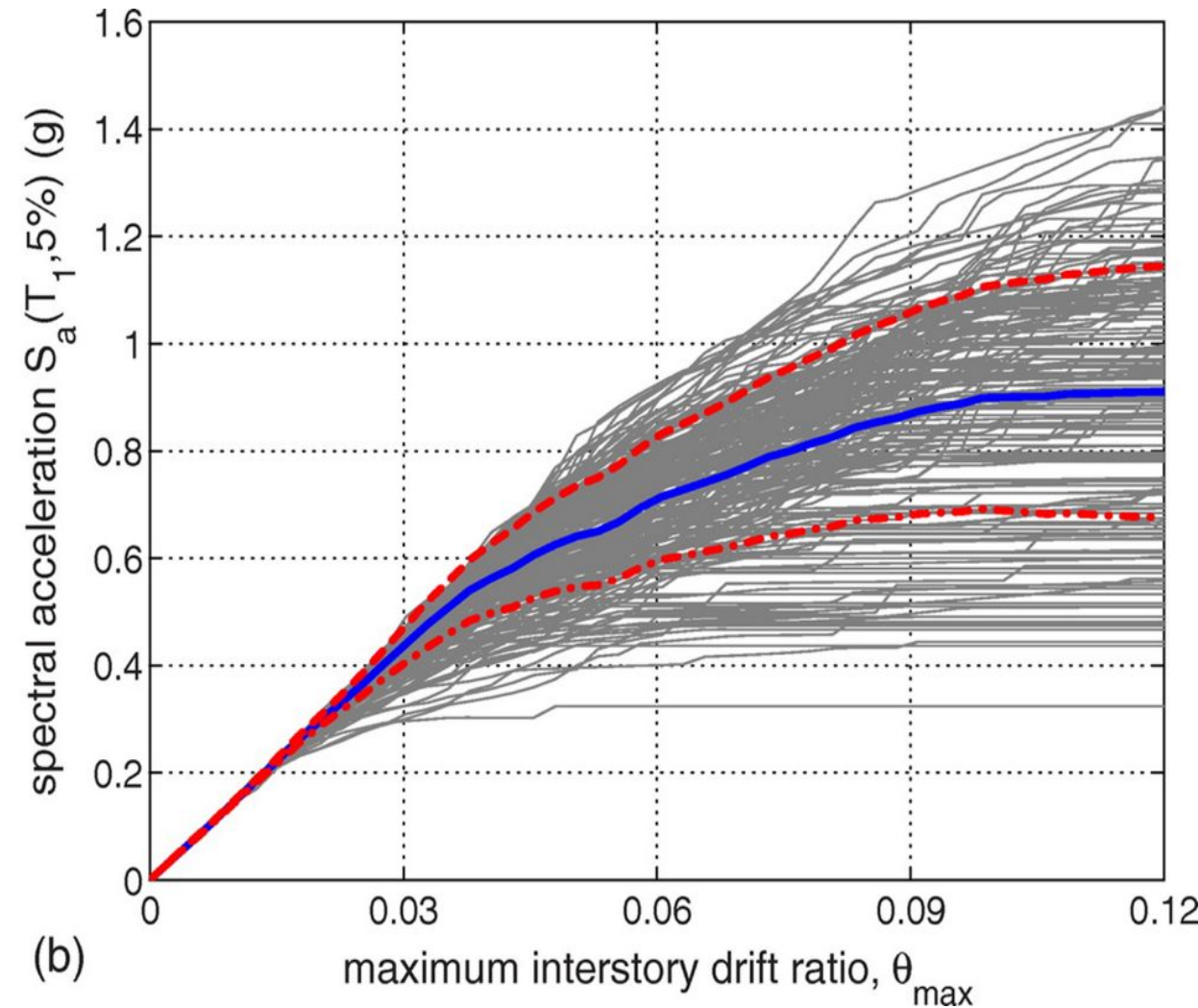
RELEVANT BUILDING SURVEYOR

A registered building surveyor who has been selected to provide independent oversight of buildings and building work throughout the construction process and upon completion of construction to ensure that buildings are safe for use, accessible and energy efficient.

Spectral acceleration (SA) is a unit measured in g (the acceleration due to Earth's gravity, equivalent to g-force) that describes the maximum acceleration in an earthquake on an object – specifically a damped, harmonic oscillator moving in one physical dimension.

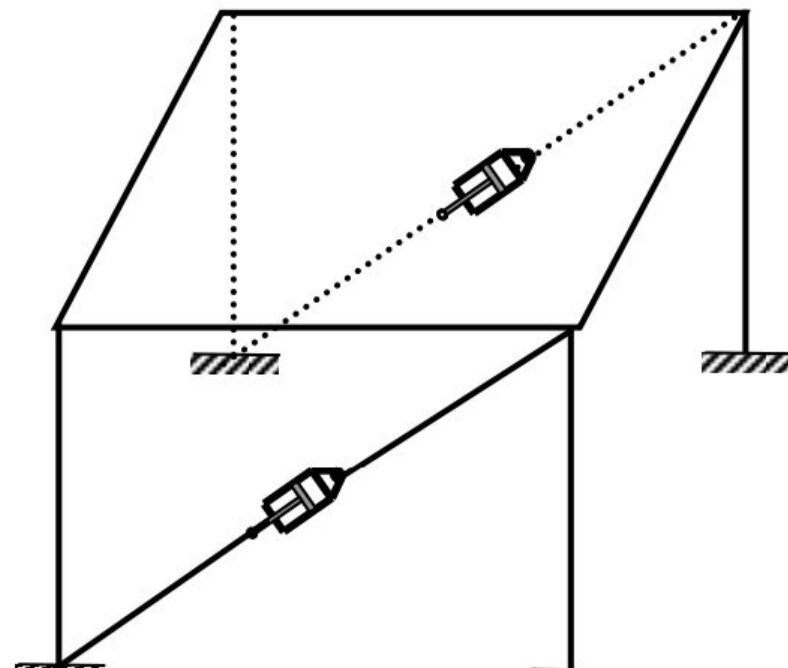


(a)



(b)

STRUCTURAL MODELLING



(a) 3-D view

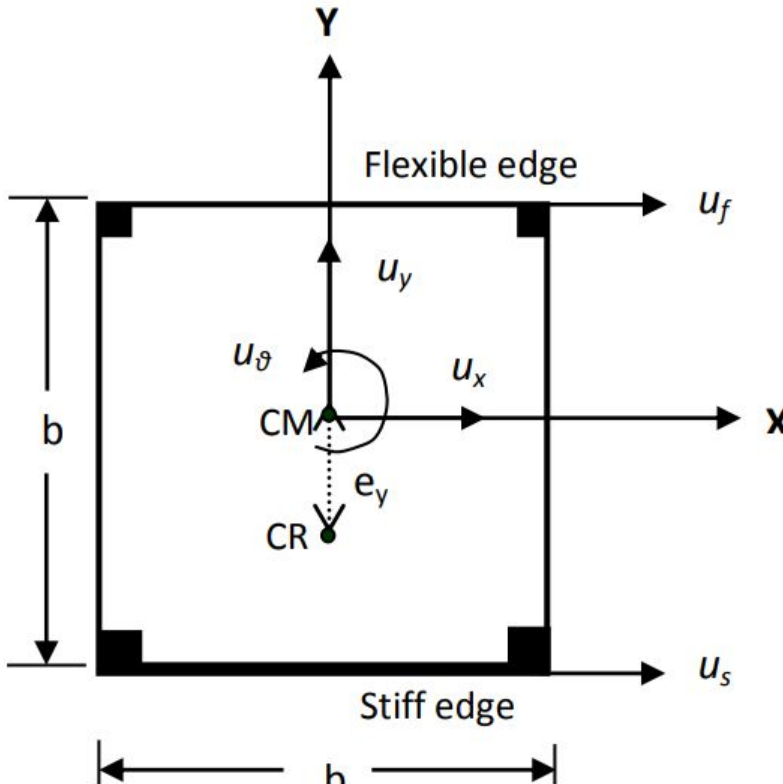


Figure 4.1. Single story plan-asymmetric building with MR dampers.

(b) Plan

A magnetorheological damper, also known as a magnetorheological shock absorber, is a damper filled with magnetorheological fluid that is controlled by a magnetic field, which is often generated by an electromagnet.

This permits the shock absorber's damping characteristics to be continually changed by altering the electromagnet's power. As the magnetic intensity rises, so does the fluid viscosity within the damper.

In addition, the system includes MR dampers installed in the bracing systems in the X-direction. The building model considered is an idealised one-story one-way plan asymmetric building consisting of rigid deck supported by structural elements (i.e. wall, columns, moment-frames, braced frames, etc.) in each of the two orthogonal directions.

The mass attributes of the system are regarded symmetric about both axes, whereas stiffness properties are only symmetric about the Y-axes. The stiffness eccentricity, e_y , is defined as the distance between CM and CR and describes the absence of symmetry in the stiffness qualities about X-axes (Figure 4.1).

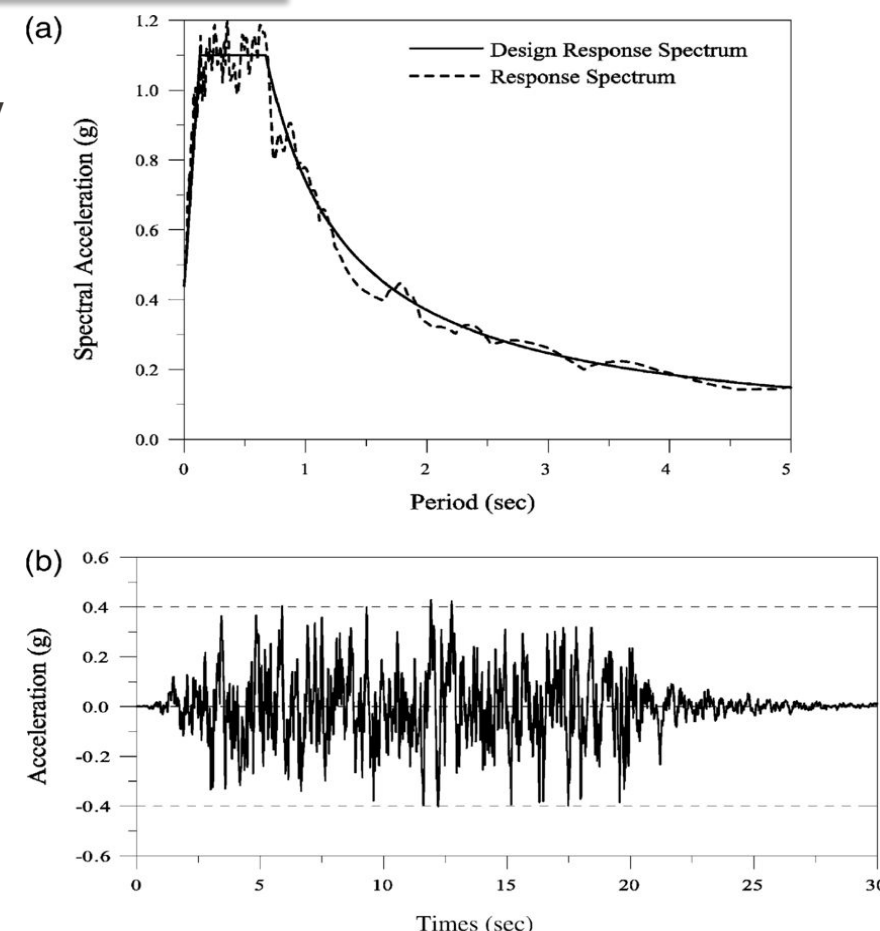
The three uncoupled natural frequencies of the system can be expressed as-

$$\omega_x = \sqrt{\frac{k_{xx}}{m}}$$

$$\omega_y = \sqrt{\frac{k_{yy}}{m}}$$

$$\omega_\theta = \sqrt{\frac{k_{\theta\theta}}{m\rho^2}}$$

where, m is the mass of the deck, k_{xx} and k_{yy} are the translational stiffness in X and Y direction respectively, $k_{\theta\theta}$ is rotational stiffness and ρ is the mass radius of gyration.



The governing equations of motion of the system in matrix form is expressed as below

$$[M]\{\ddot{u}\} + [C]\{\dot{u}\} + [K]\{u\} = [D]\{f_m\} - [M][r]\{\ddot{u}_g\}$$

where, M , C , and K are mass, damping, stiffness matrices of the building respectively; f_m is the vector consisting of forces in the MR dampers; D is the damper location matrix; u is the relative displacement vector with respect to the ground, r is the influence coefficient vector, and \ddot{u}_g is the earthquake ground acceleration. The M and K matrices are expressed as

$$M = \begin{bmatrix} m & 0 & 0 \\ 0 & m\rho^2 & 0 \\ 0 & 0 & m \end{bmatrix}$$

$$K = \begin{bmatrix} k_{xx} & k_{x\theta} & k_{xy} \\ k_{\theta x} & k_{\theta\theta} & k_{\theta y} \\ k_{yx} & k_{y\theta} & k_{yy} \end{bmatrix}$$

Researchers have investigated the application of various control devices for seismic response control of torsionally coupled systems; Jangid and Datta (1997) examined the performance of Multiple Tuned Mass Dampers (MTMD) for torsionally coupled system through parametric study. The effect of supplemental damping on the edge deformation of a asymmetric-plan systems was investigated by Goel (1998, 2000), Lin and Chopra (2001) showed that the reduction in earthquake response of the system achieved by supplemental damping is strongly influenced by its planwise distribution. Date and Jangid (2001) investigated the effectiveness of active control system using a structural model of a one story torsionally coupled building.

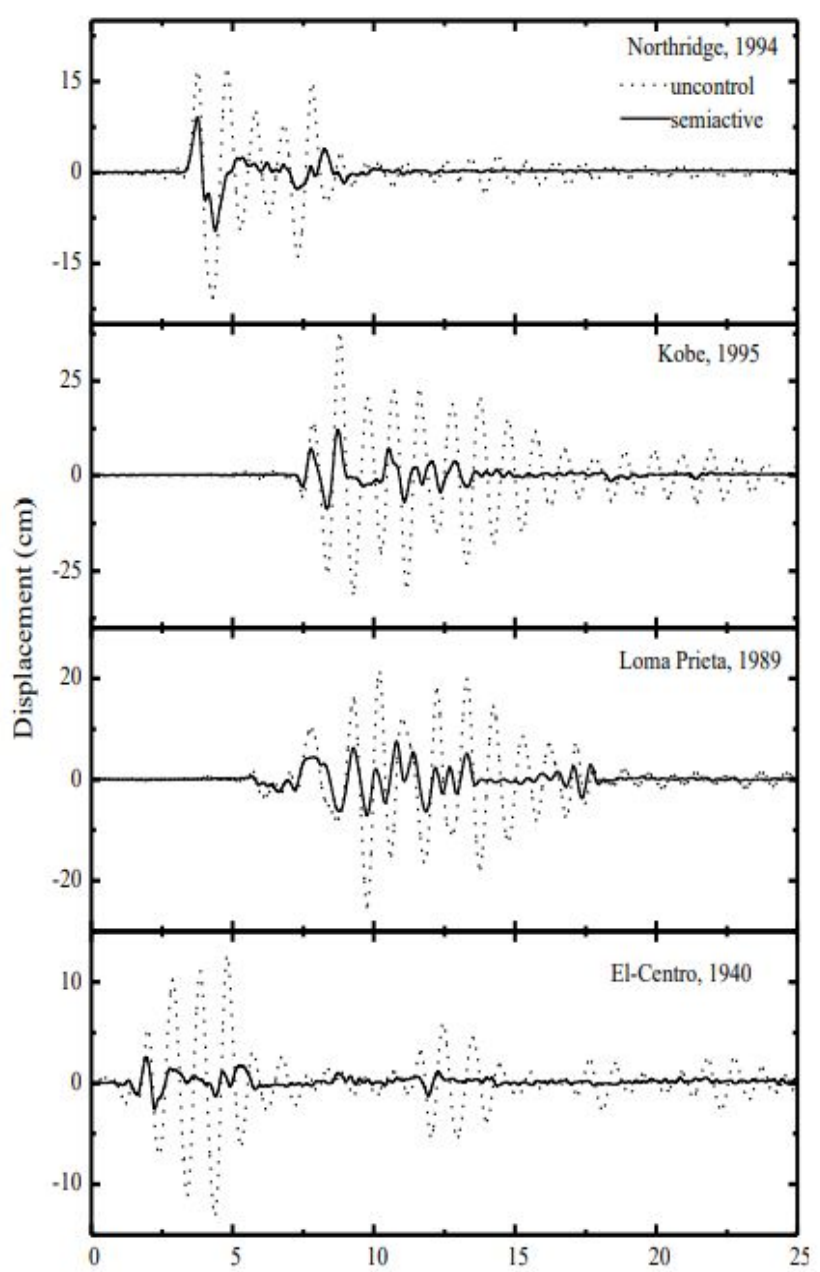


Figure 4.2. Time variation of flexible edge displacement.

($V_{\max} = 1.5V$, $n_1 = 0.1$ & $n_2 = 0.1$)

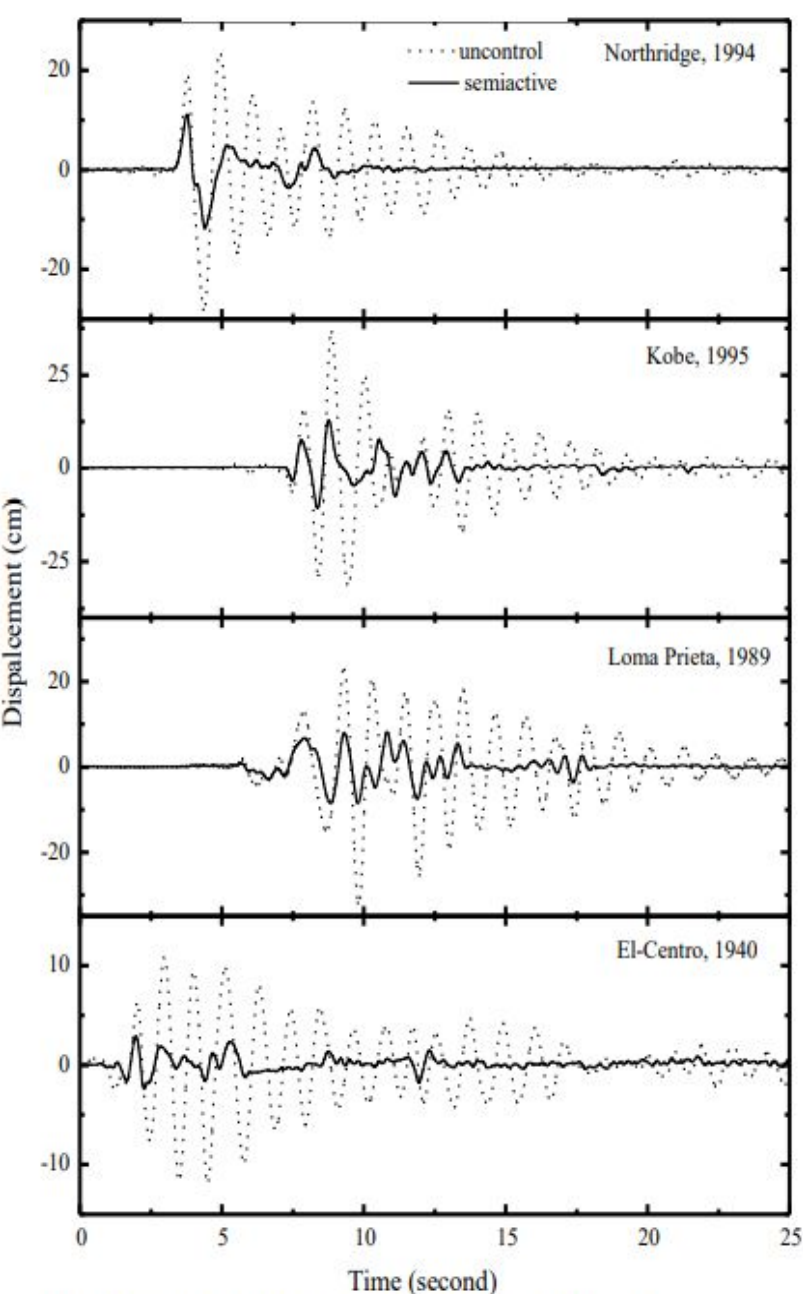


Figure 4.3. Time variation of flexible edge displacement.

($V_{\max} = 1.5V$, $n_1 = 0.1$ & $n_2 = 0.1$)

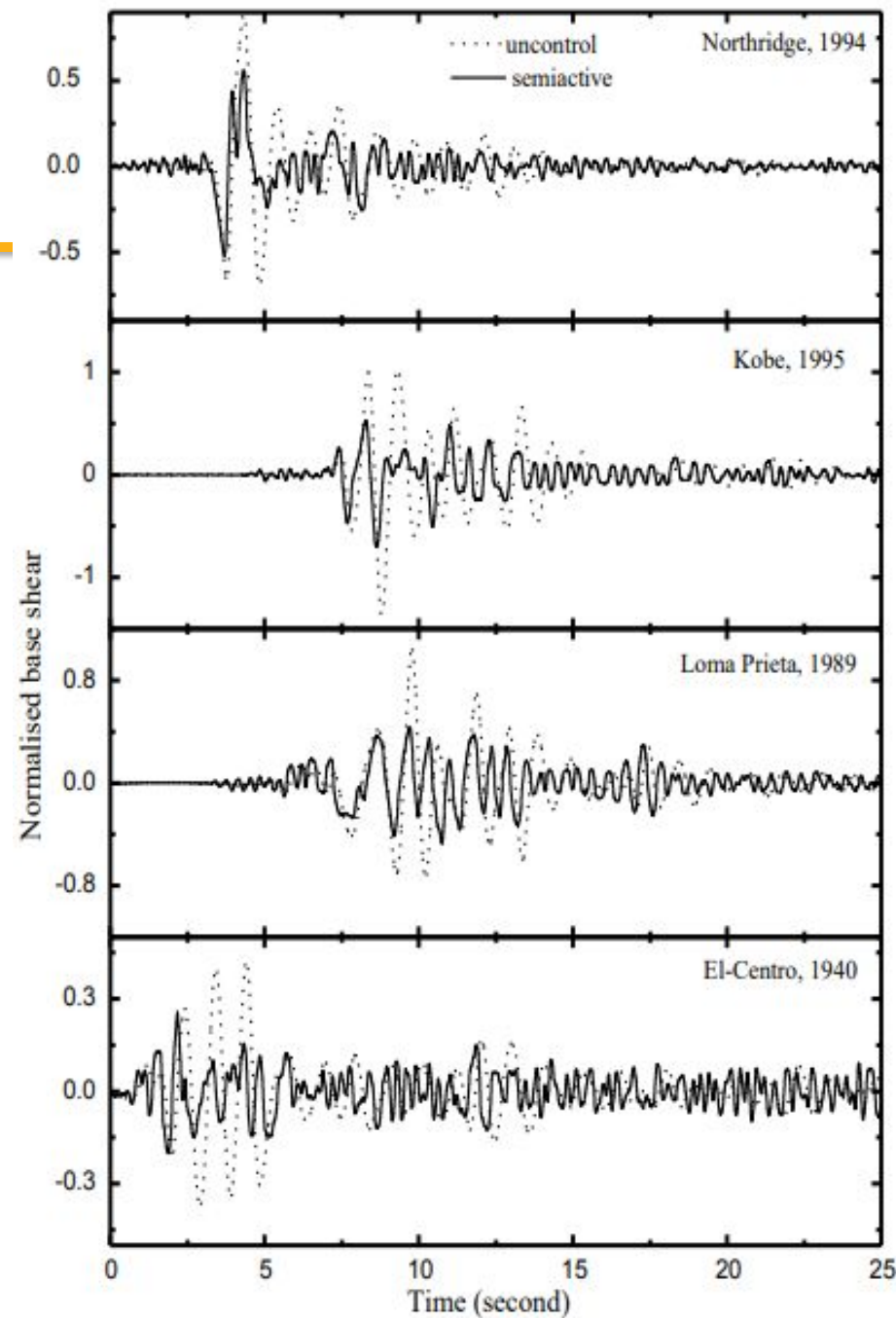


Figure 4.4. Time variation of base shear

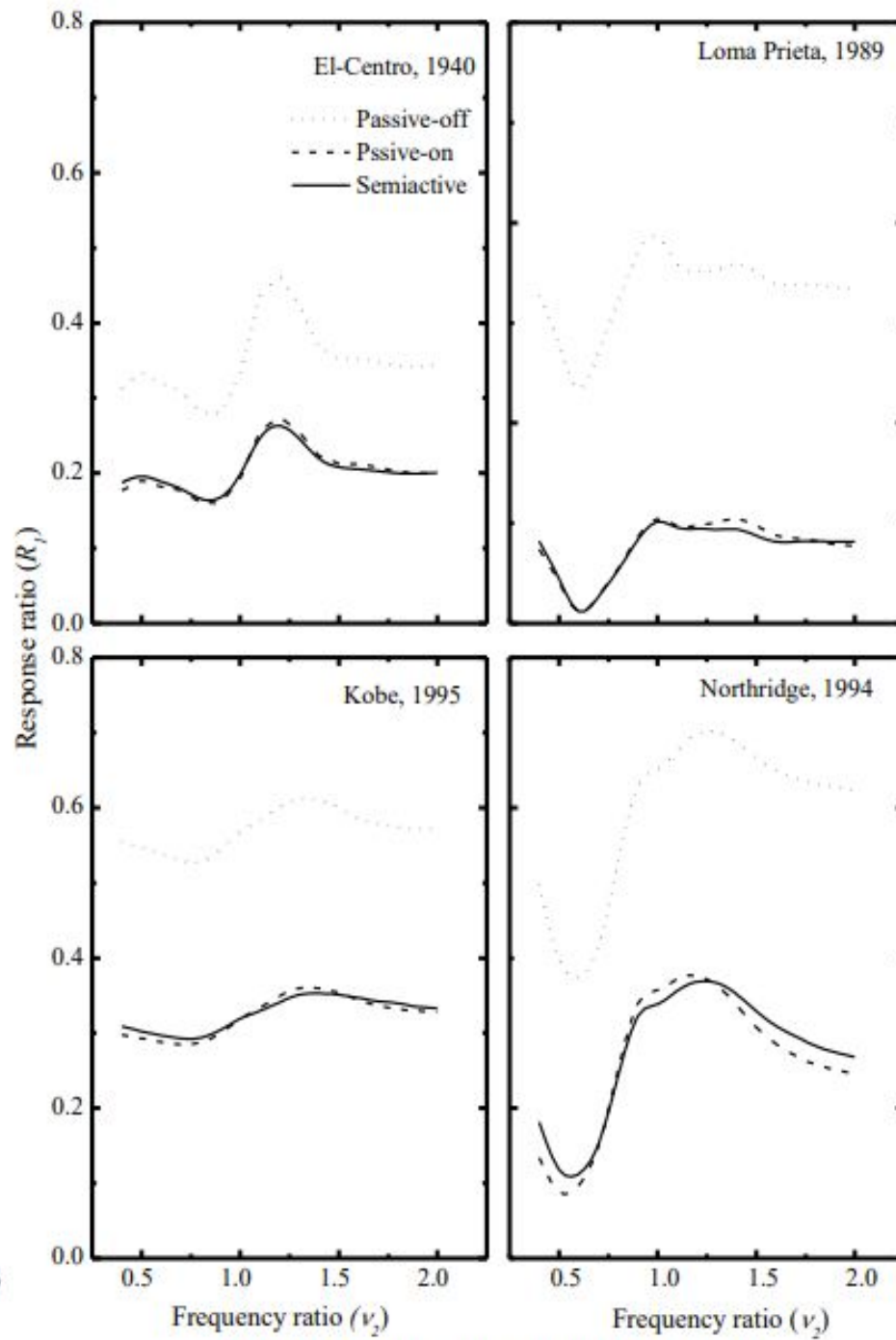


Figure 4.5. Peak displacement of flexible edge

**Passive off here
means negative
stiffness
(superior
performance)**

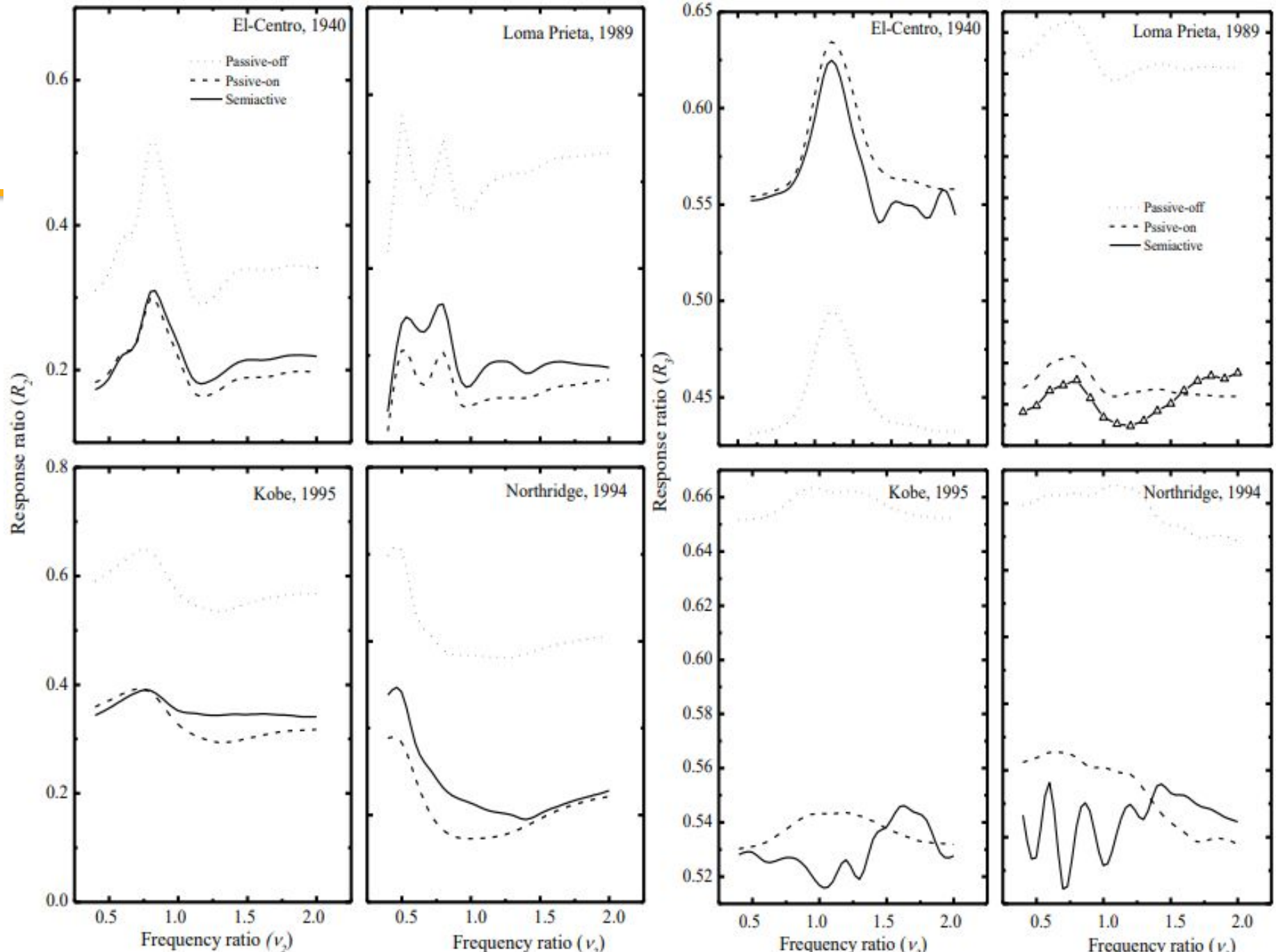


Figure 4.6. Peak displacement of stiff edge ($v_i = 0.1$)

Figure 4.7. Peak normalised base shear ($v_i = 0.1$)

**Passive on here
means positive
stiffness (poor
performance)**

PBSD procedure in STAAD Pro Advanced

Following Nonlinear Static Analysis

The study considers three structural steel frames of G+3 storey I moment frame, (ii) braced frame with external concentric diagonal bracing (bracing section –ISMC100), and (iii) braced frame with internal diagonal bracing (bracing section –ISMC100) at optimal position, as shown in fig 2 (a), (b), and (c), respectively.

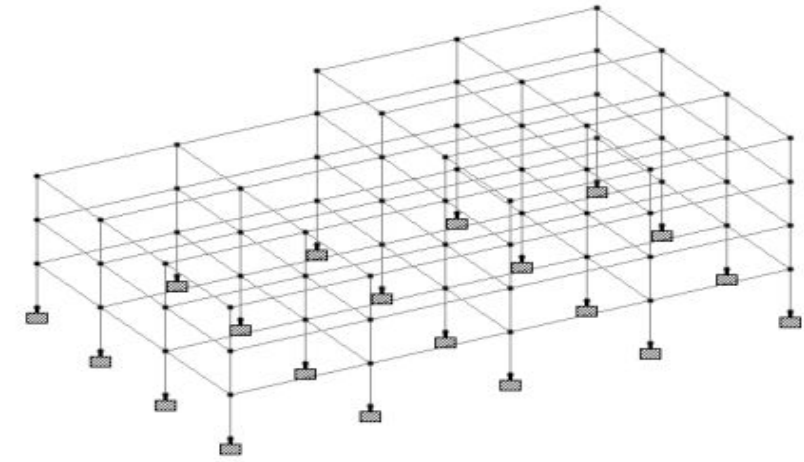
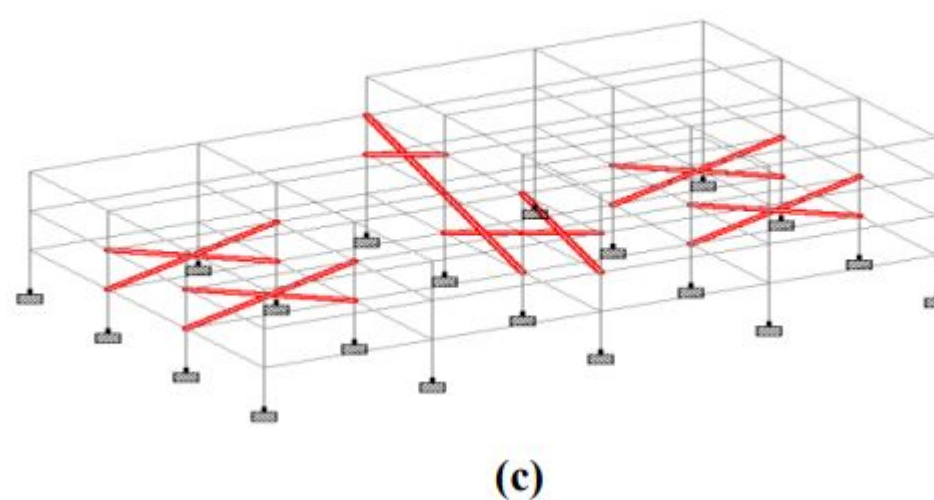
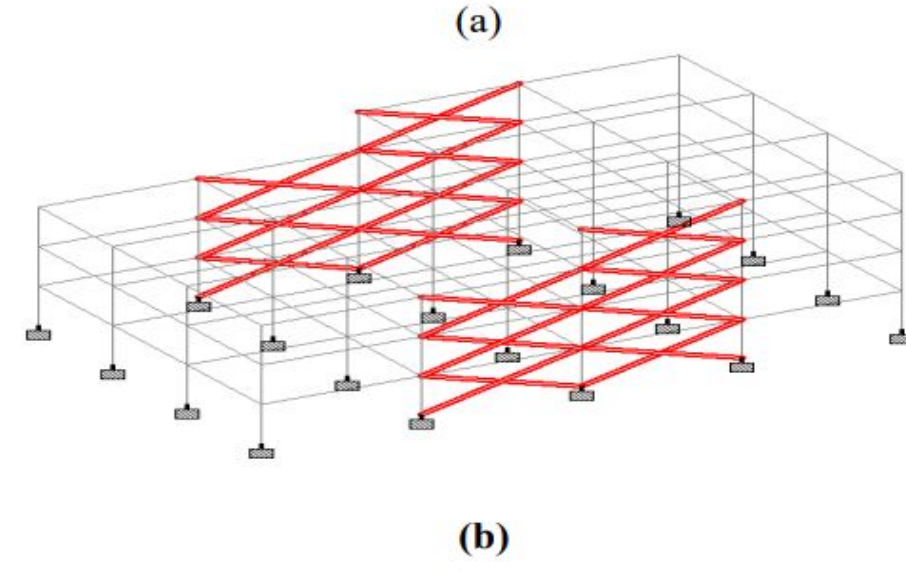


Fig 2.



(c)

Structural Modeling of Steel Frames in STAAD Pro. Advanced, (a) moment frame;
(b) braced frame with external concentric diagonal bracing;
(c) braced frame with internal diagonal bracing

The geometry of all three structural steel frames is shown in Table 1.

The cross sectional details of the beams and columns employed in all three frames are shown in Table 2. The strong column weak beam idea is considered while assigning steel sections to column and beam.

The modulus of elasticity of the steel used to produce the 4-Storey braced frame is 199947.9611 N/mm², the Poisson's ratio is 300E-3, the density is 283E6 kip/in³, and the α/oF is 6.5E6.

Table- I: Geometry of Braced Steel Frame

Floor	Height (m)	Length (m)	Width (m)
Ground Floor	3.048	28.48	18.28
1st Floor	3.048	28.48	18.28
2nd Floor	3.048	28.48	18.28
3rd Floor	3.048	14.124	18.28

Table- II: Size of Steel Cross Section Details for Existing 4-Storey Braced Steel Frame

Model	Storey/ Floor	Column		Beam	
		Exterior	Interior	Exterior	Interior
4-Storey	4	ISHB350H	LSLB450	ISHB200	ISHB200
	3	ISHB350H	LSLB450	ISHB200	ISHB200
	2	ISHB350H	LSLB450	ISHB200	ISHB200
	1	ISHB350H	LSLB450	ISHB200	ISLB300

As illustrated in fig 3, each frame has its own self weight and life load of 3kN/m.

To do the pushover analysis in STAAD Pro. advanced, self weight and live weights were applied under gravity load conditions.

Figure 3 depicts the self-weight of the structure in red, and blue coloured arrows pointing downward illustrate the gravity load of 3Kn/m operating in the global Y direction.

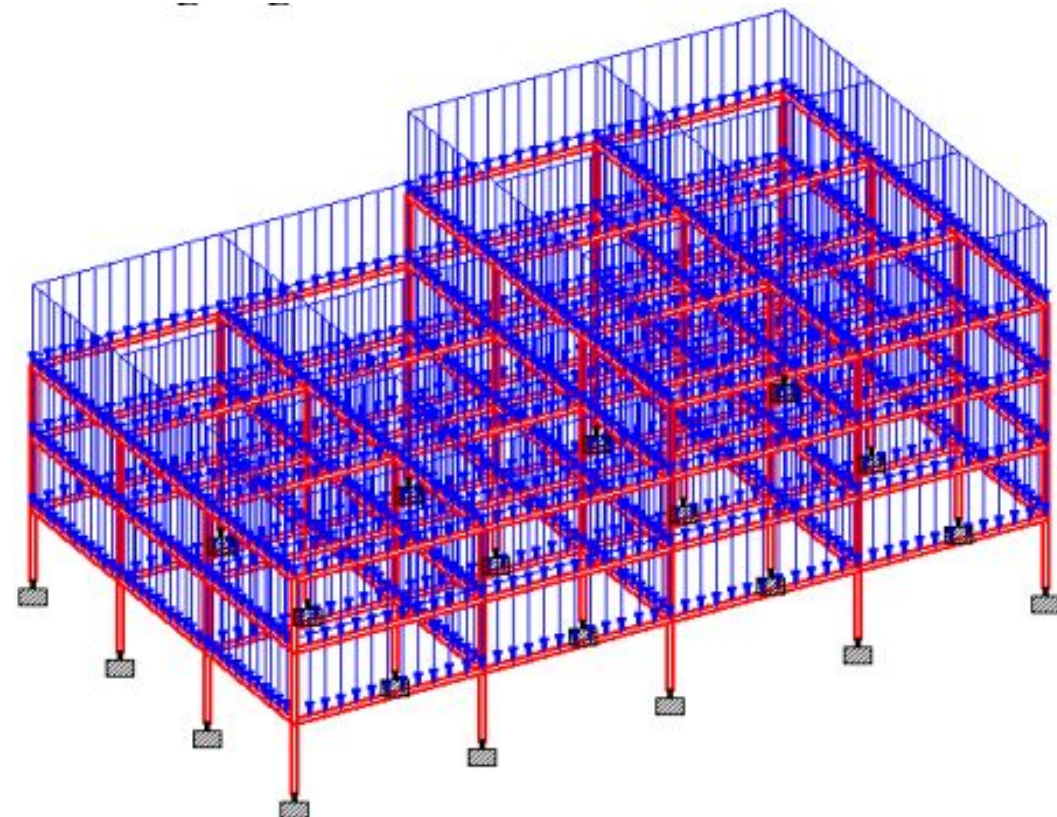


Fig.3. Gravity Loading on Structural Steel Frame for Pushover Analysis

PERFORMING PUSHOVER ANALYSIS

STAAD Pro. advanced is used to do pushover analysis on each structural steel frame of the G+3 story. While performing non-linear static analysis, the following steps were taken.

While performing pushover analysis in STAAD Pro, define the type of frame. Advanced frame types should be defined initially. Moment frame is the frame type for the first frame, and braced frame is the frame type for the second and third frames.

Geometric Non-linearity: In regular buildings, some structural damage is allowed during intense earthquake shaking, even though no collapse must be guaranteed. This indicates that nonlinearity will emerge in the building's overall response. As a result, the geometric non linearity is taken into account when assessing all three steel frames. The geometric nonlinearity convergence is set to 0.254mm, and the number of iterations for geometric nonlinearity is set at 50.

Defining Loads: In the gravity loading example, loads are defined. Gravity loads are made up of dead loads and (in most cases) most live loads. Each steel frame is given a live load of 3kN/m, as indicated in fig 3.

Defining acceptance criteria: Performance characteristics that regard all elements to be primary. As a result, the performance points are as illustrated in Figure 4's curves. IO is the distortion that caused persistent, visible damage in the experiment but did not exceed 0.67 times the LS deformation limit. The distortion at point 2 on the curves is 0.75 LS. CP is the curve deformation at point 2 that is less than 0.75 times the curve deformation at point 3.

Performance Based Seismic Analysis of Steel Frames

Component force v/s
deformation curves from
FEMA 356

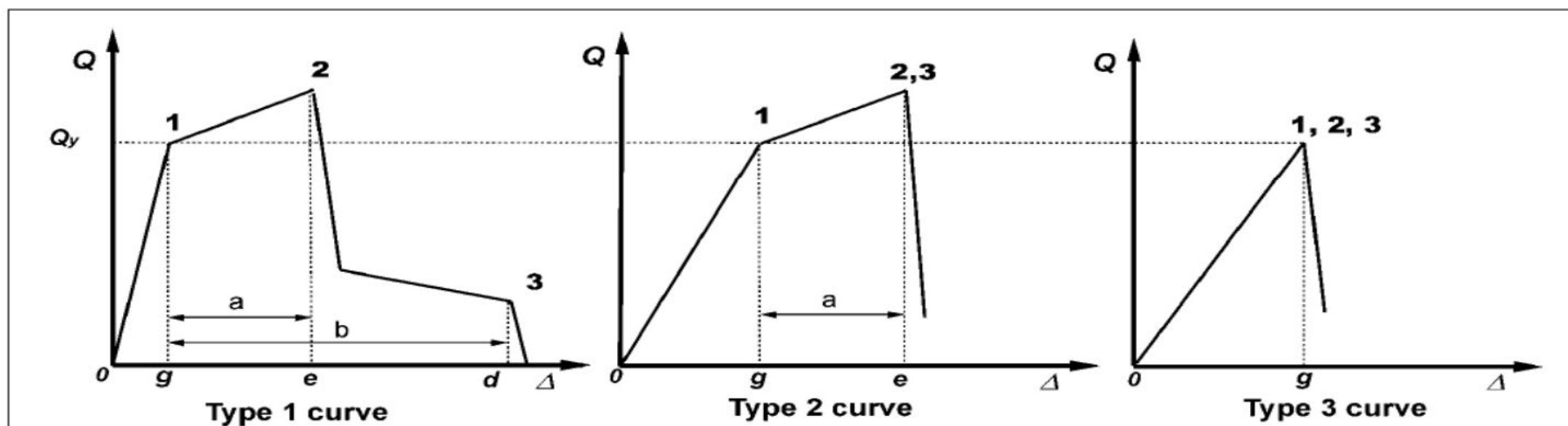
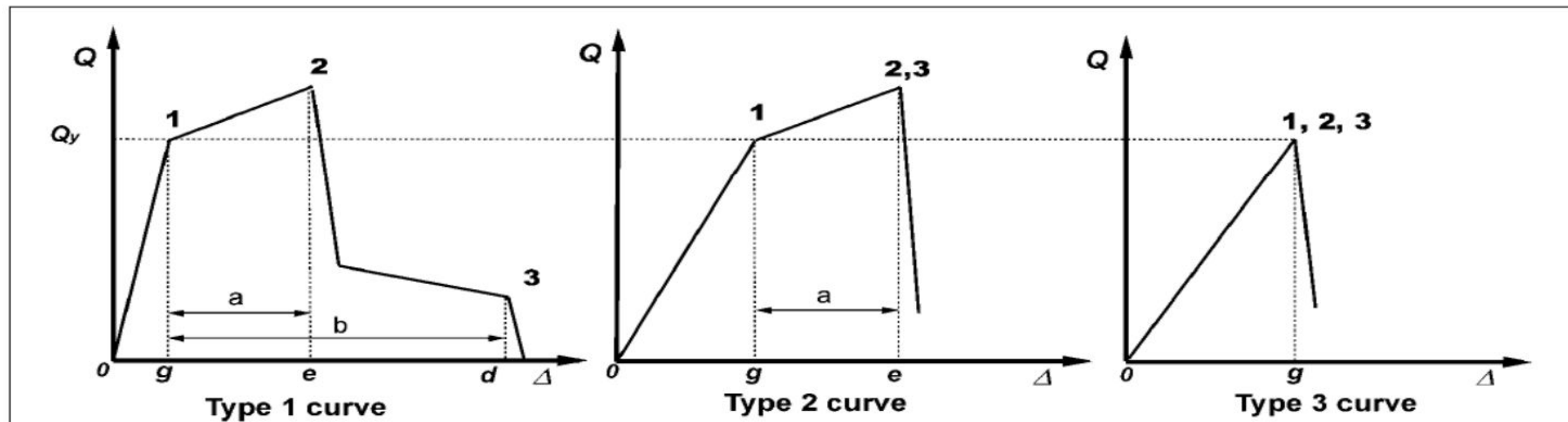


Fig 4.

Defining Solution Control: A defined base shear or a defined displacement at a controlled joint can be used to do the analysis. As previously described in step 4 of doing pushover analysis, the push up to defined base shear technique is employed here.

Performance Check: The performance of all three G+3 structural steel frames was determined by pushover analysis, with comparisons of base shear, displacement, capacity curve, and plastic hinges computed to determine which structure satisfies the requisite performance under earthquake stress.



RESULT

Performance of Moment Frame: After completing pushover analysis on the G+3 storey steel frame, it performed linearly up to a base shear of 135.09KN, then nonlinearly as the base shear increased. As indicated in figure 5, the first plastic hinge is formed in column 9 and column 12.

At that point, the performance level is IO. When the base shear is increased to 3758.82 KN, blue coloured plastic hinges develop at columns 5, 8, 13, and 16, as illustrated in fig 6, indicating that the structure is between the IO and LS performance levels.

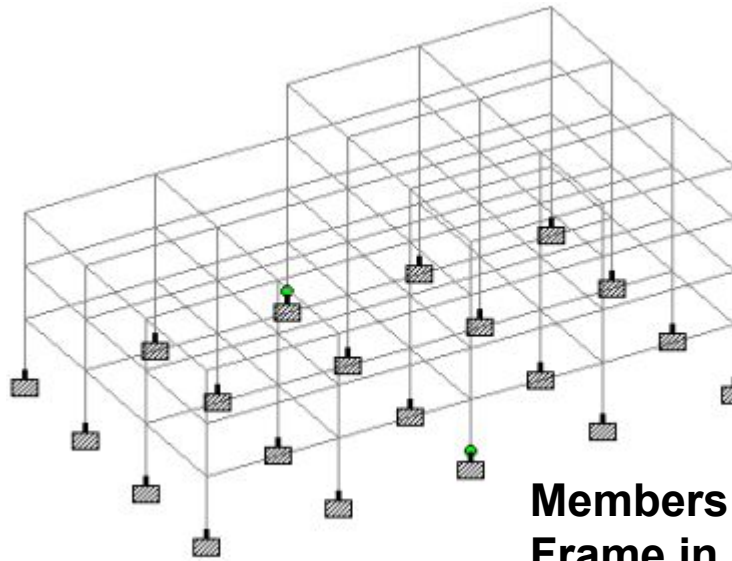


Fig 5.

Members of Moment Steel Frame in IO Performance Level

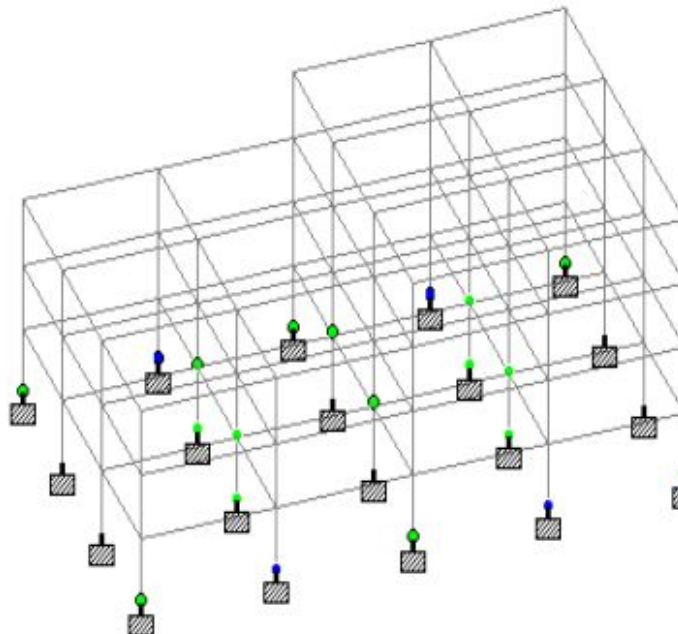


Fig 6.

Members of Moment Steel Frame in IO-LS Performance Level

As the base shear reached 4218KN, pink coloured plastic hinges began to appear in column 5, 8, 13, and 16, as seen in fig 7, indicating that those structural components are performing at the LS-CP level.

As illustrated in fig 8, red coloured plastic hinges started forming into column 5, 8, 13, and 16 at the base shear 4392.60 KN, indicating that those structural components are in the CP level.

**Members of Moment Steel
Frame in LS-CP**

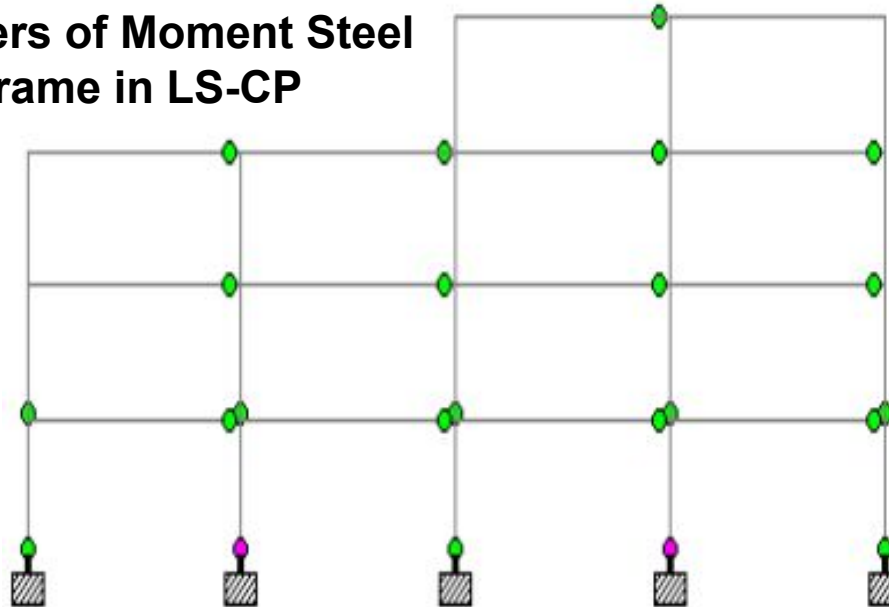


Fig 7.

**Members of Moment Steel
Frame in CP**

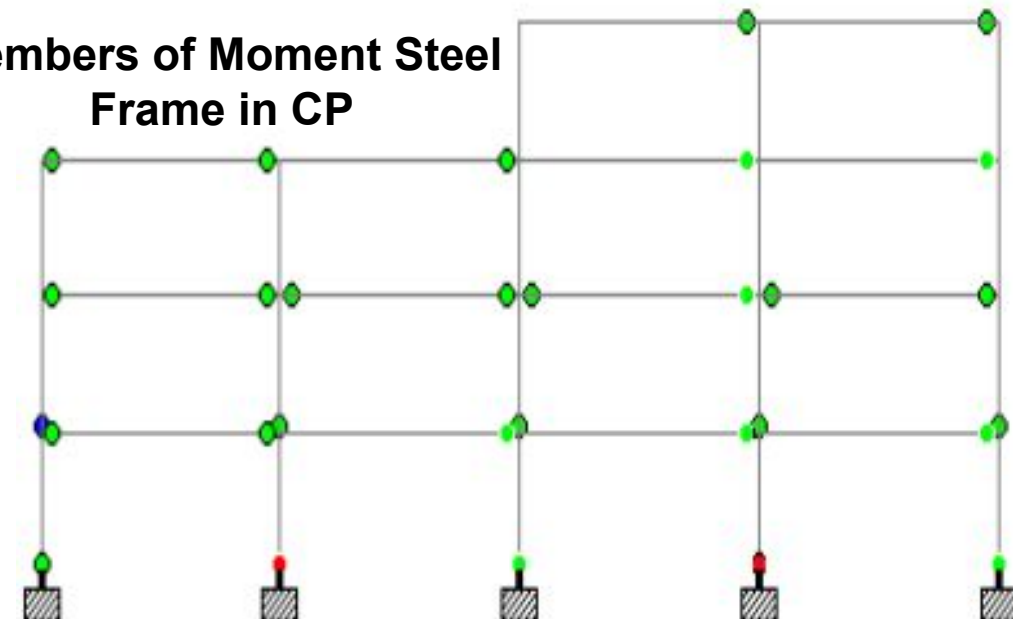


Fig 8.

Immediate occupancy (IO), life safety (LS) and collapse prevention (CP)



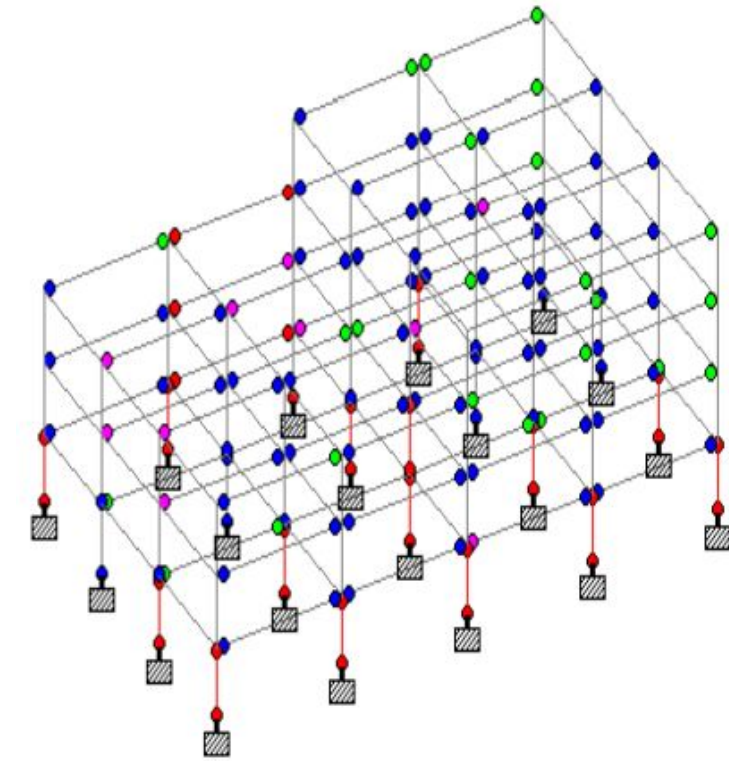
Base shear began redistributing to assess the performance of other structural parts when the member of the structure reached the CP performance threshold. No members had collapsed till that point. Columns 5 and 8 of the first member failed at the base shear 4260.87KN, as indicated by the red colouring.

However, the complete structure was not affected because the maximum columns are within the IO performance level, as illustrated in fig. The highest number of beams and columns are in the CP and LS levels after distributing and redistributing base shear up to the push load step 173, but some of them are collapsed as shown in fig when the redistributed base shear was 2380.60 KN.

After that, the entire structure will fall because the base storey's maximum number of columns has failed, as seen in fig 9.

The capacity curve for a moment frame is given in fig 10, where the X-axis represents the displacement at the roof caused by base shear, which is displayed on the Y-axis.

Capacity Curve of Moment Frame



Members of Moment Steel Frame Failed in Pushover Analysis

Fig 9.

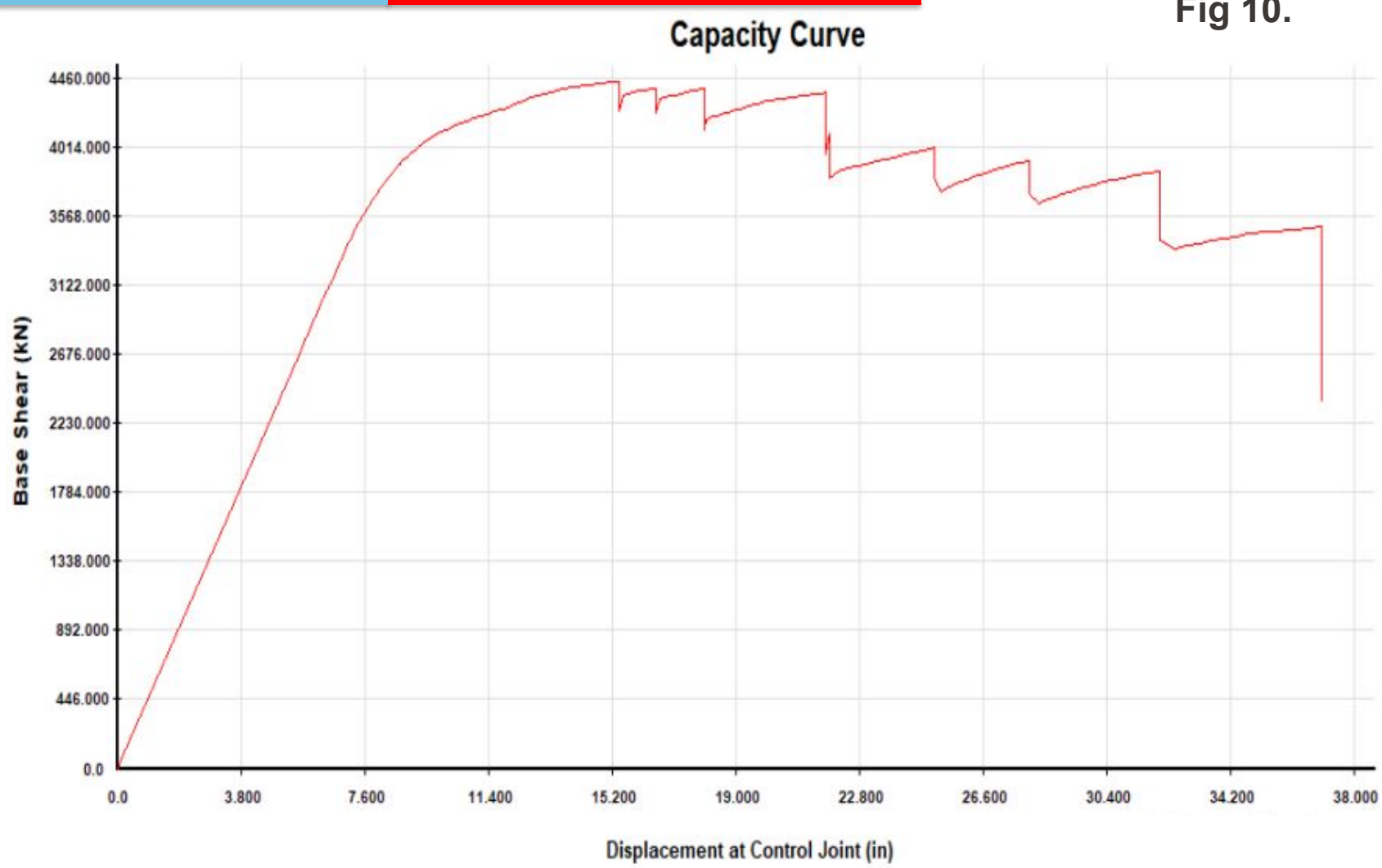


Fig 10.

Performance of Externally Braced Frame: The static nonlinear process was used to assess the G+3 storey frame, which functioned linearly up to the base shear of 137.70KN. As illustrated in fig11, when the base shear is 3879.86KN, column 6,7,14, and 15 are in the IO performance level, with green coloured plastic hinges.

When the base shear reached 5161.37KN, column 10 and 11 were in the IO – LS performance level, as shown in fig 12. When the base shear reached 5406.2794KN, column 10 and 11 were in the LS-CP performance level, as shown in fig 12.

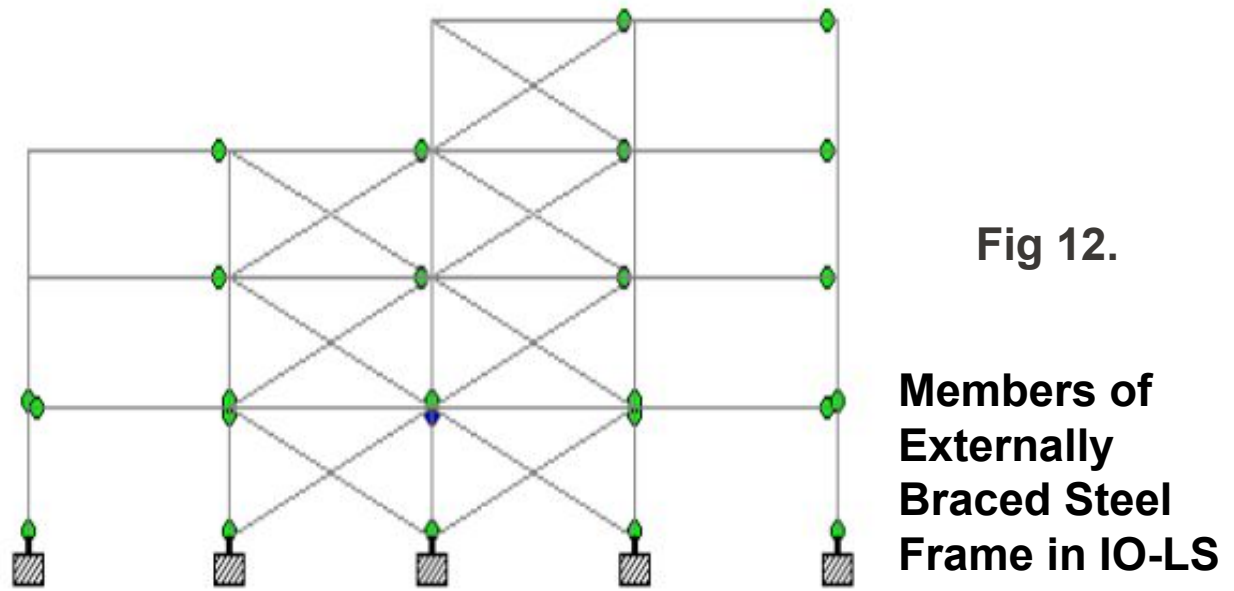
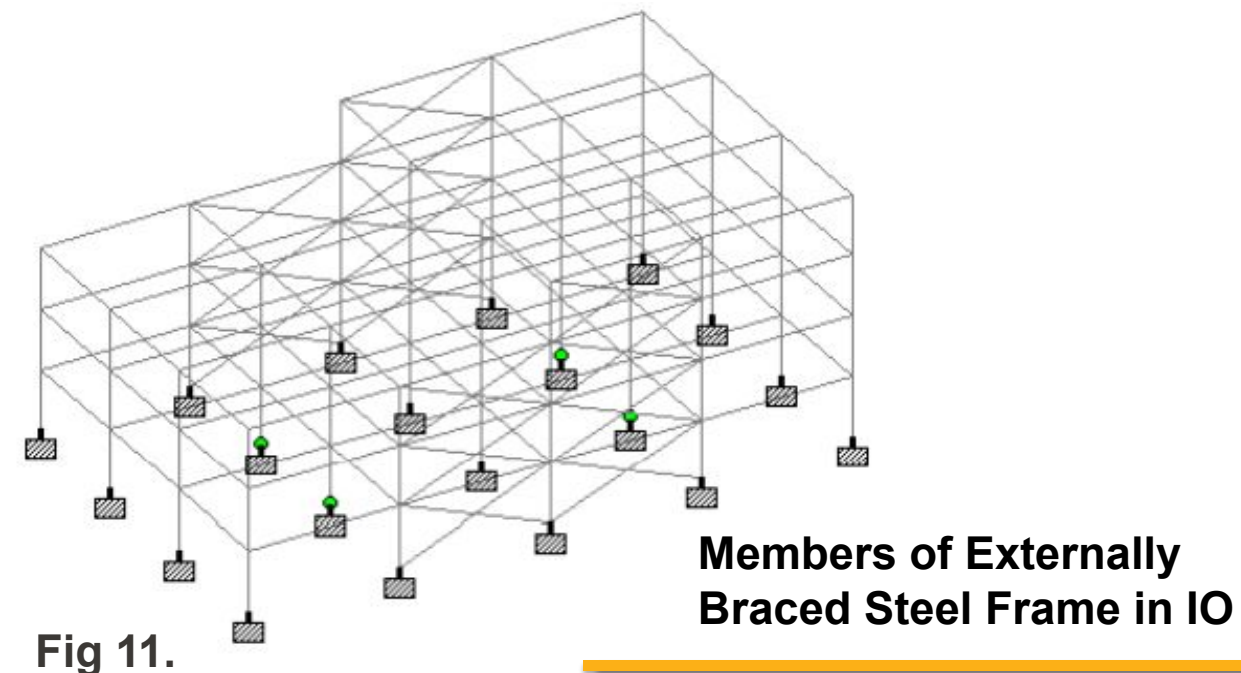
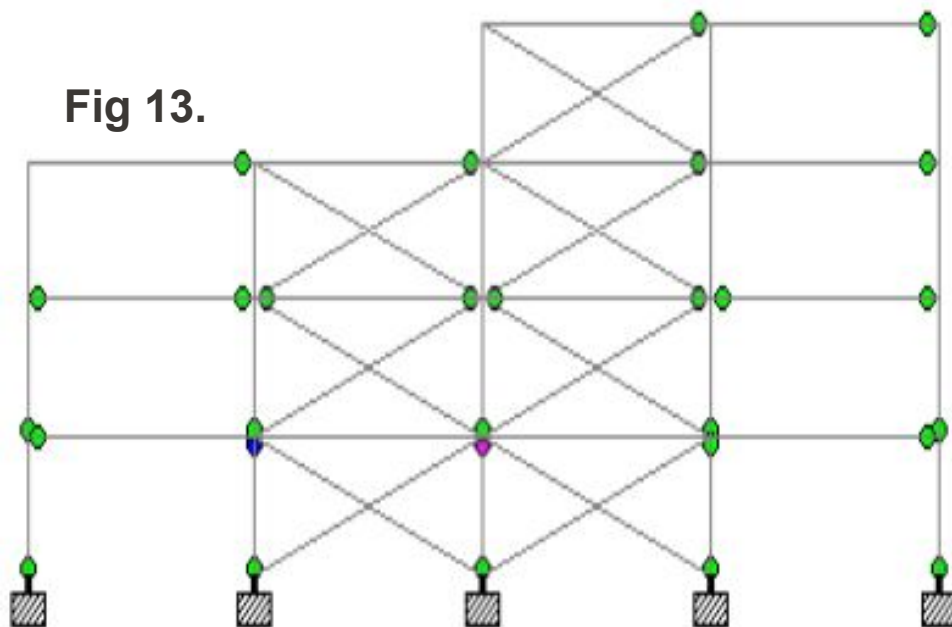


Figure 13 shows the complete CP level when the base shear is 5545.04KN.

As illustrated in fig 14, the bracing supplied began to fail when the base shear was 5636.119KN. External bracings boost the structure's lateral load carrying capacity, but displacement increases as well, resulting in structural failure.

The base shear was then redistributed up to the push load stem 231 and the basement's maximum columns failed at base shear 6039.11KN.

Fig 13.

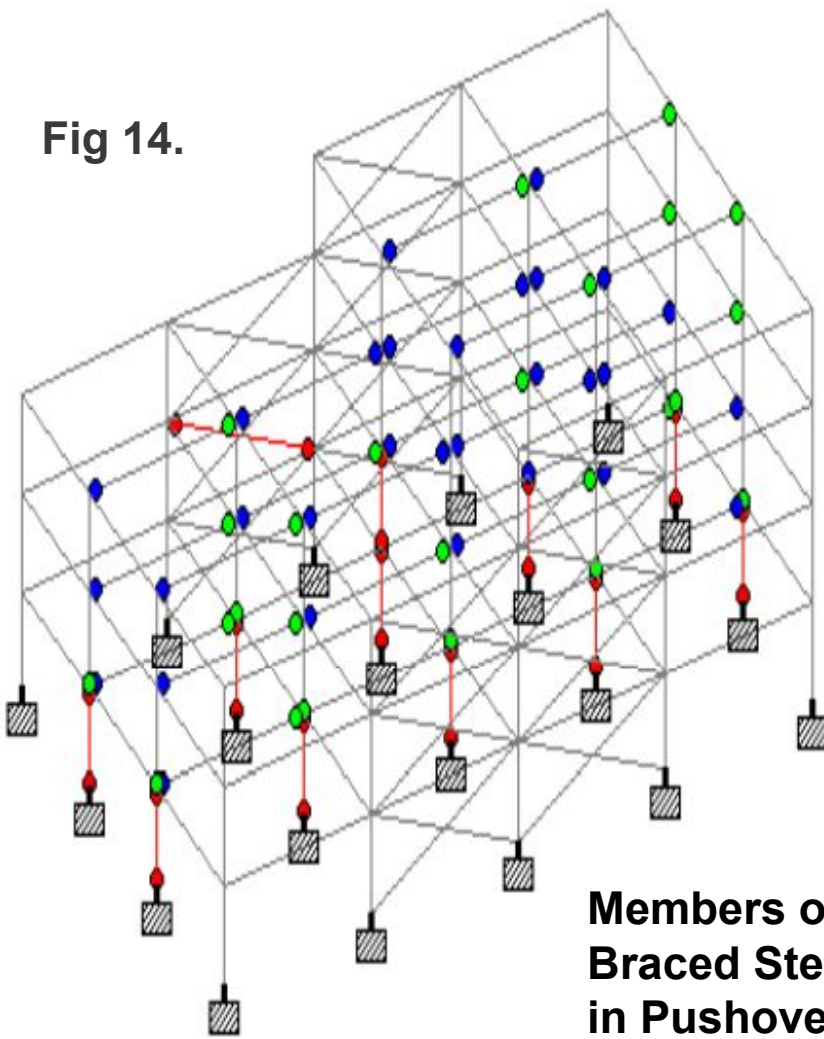


**Members of Externally
Braced Steel Frame in
LS-CP**

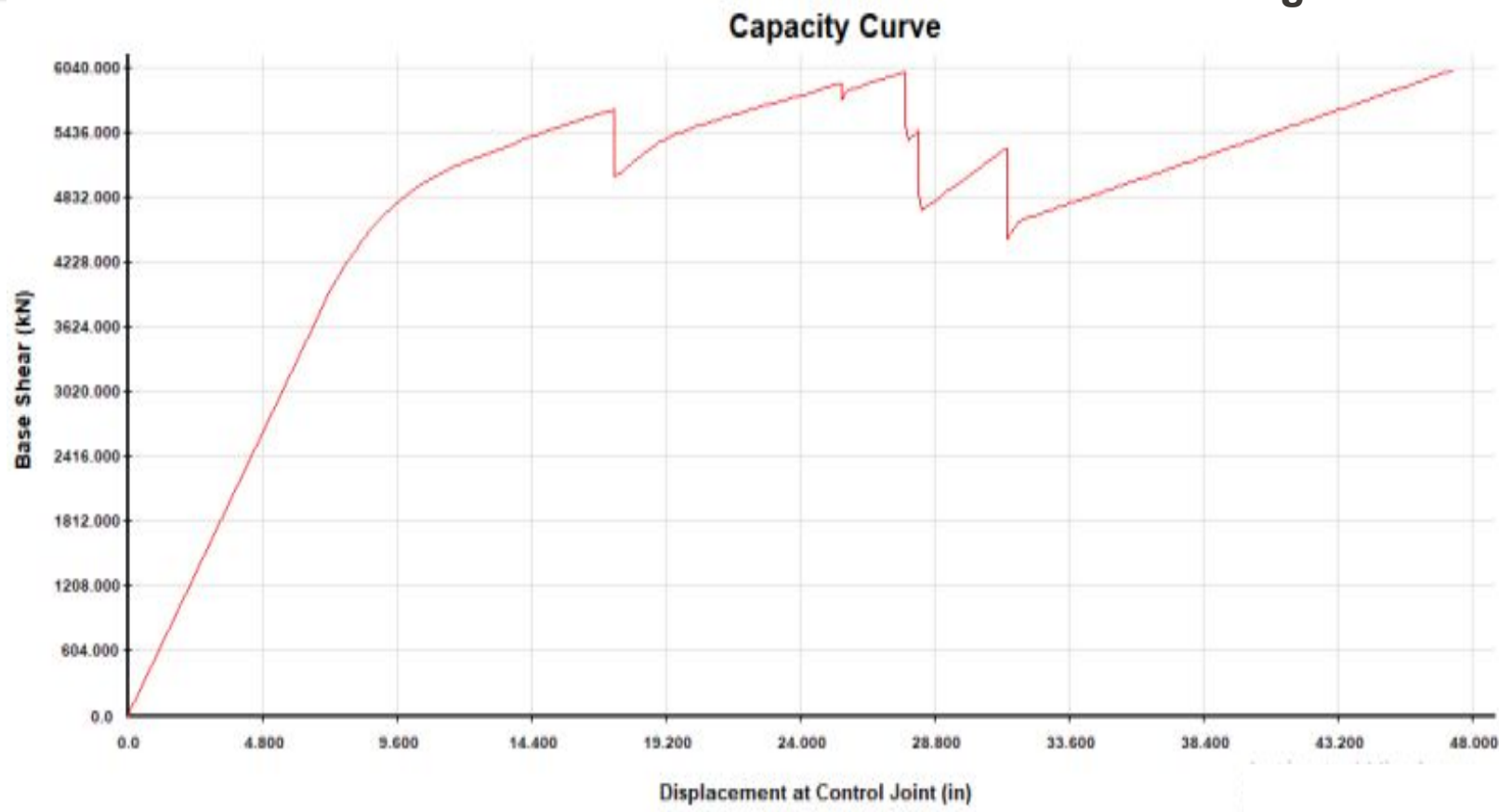
The entire structure will then collapse. Figure 15 depicts the capacity curve for this period.

Fig 15.

Fig 14.



**Members of Externally
Braced Steel Frame Failed
in Pushover Analysis**



Capacity Curve for Externally Braced Steel Frame

Performance of Internally Braced Frame at Optimal Position: Following the findings of the previous two frames, the third frame was developed with internal bracings in place to prevent the failure of members seen in the first and second frames. For that goal, various bracing positions were tested, and the frame depicted in this study with the ideal bracing position yielded the most accurate collapse prevention findings.

As demonstrated in fig 16, column 5,8,9,12,13, and 16 in a G+3 internally braced steel frame are in IO performance level ate base shear 3536KN. When the base shear is 4517.66 KN, column 27 and 31 attain the IO-LS performance level, as illustrated in fig 17.

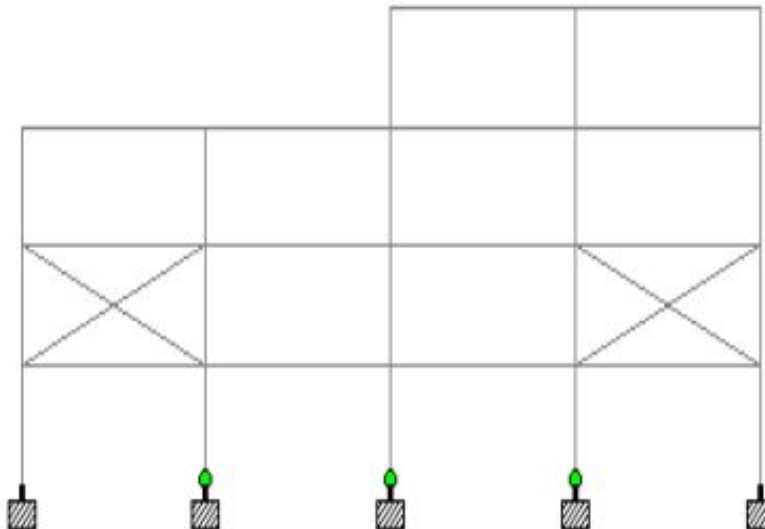


Fig 16.
Members of
Internally Braced
Steel Frame in IO

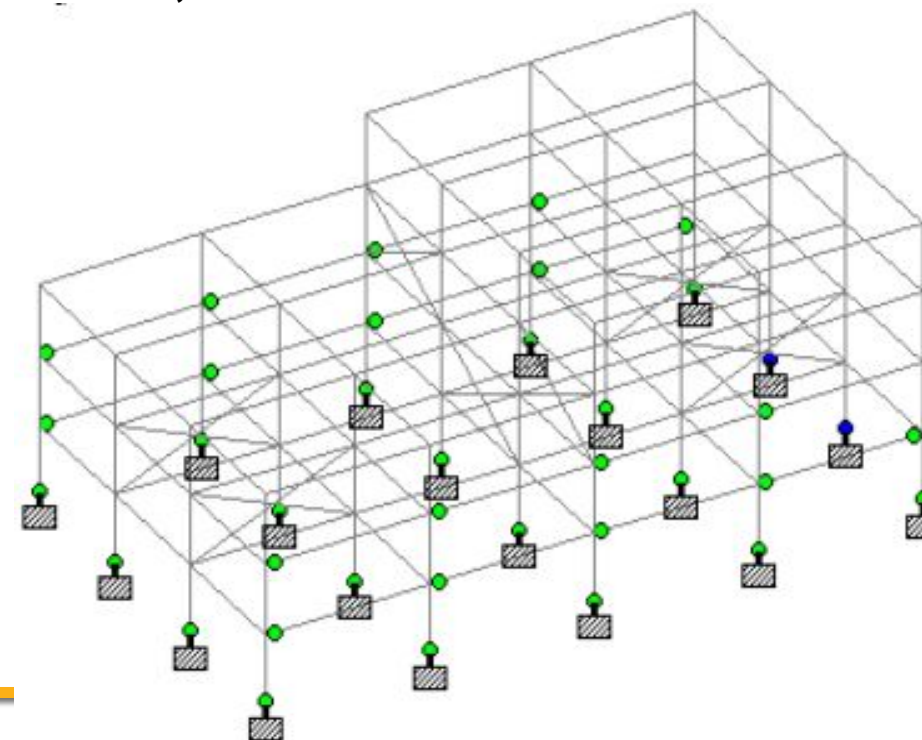


Fig 17.

Members of
Externally
Braced Steel
Frame in
IO-LS

When the base shear is 5128.46KN, column 10 and 11 in fig 18 are I LS-CP levels. At base shear 5222.86KN, the same columns were the first in the entire structure to exceed CP level. In this design, the structure's base shear bearing capacity is improved, while its displacement is reduced as compared to an externally braced frame. As a result, the construction is safe.

After completing all of the push load steps, it was discovered that no members had failed. Only columns 10 and 11 were in the CP level, but the rest of the structure was secure. Figure 19 depicts the capacity curve.

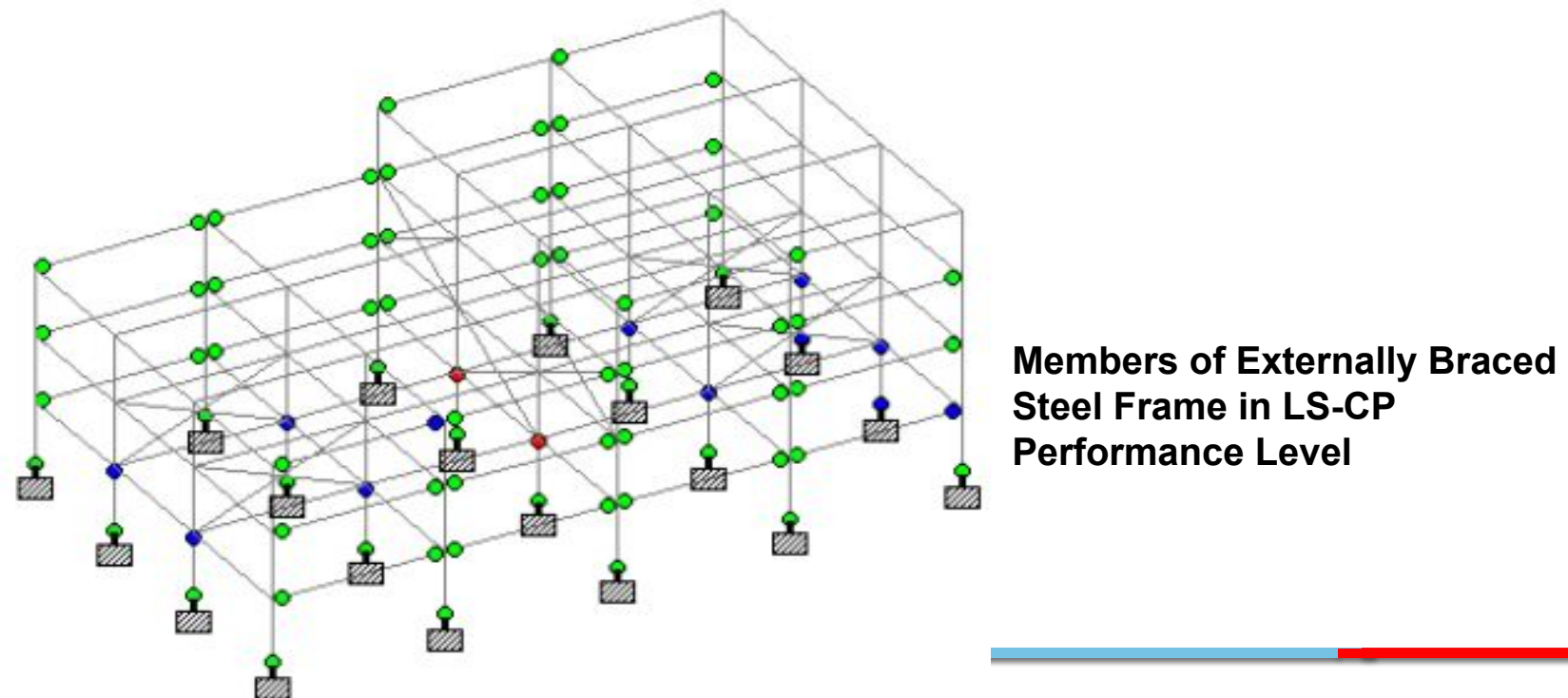


Fig 18.

Capacity Curve for Externally Braced Steel Frame

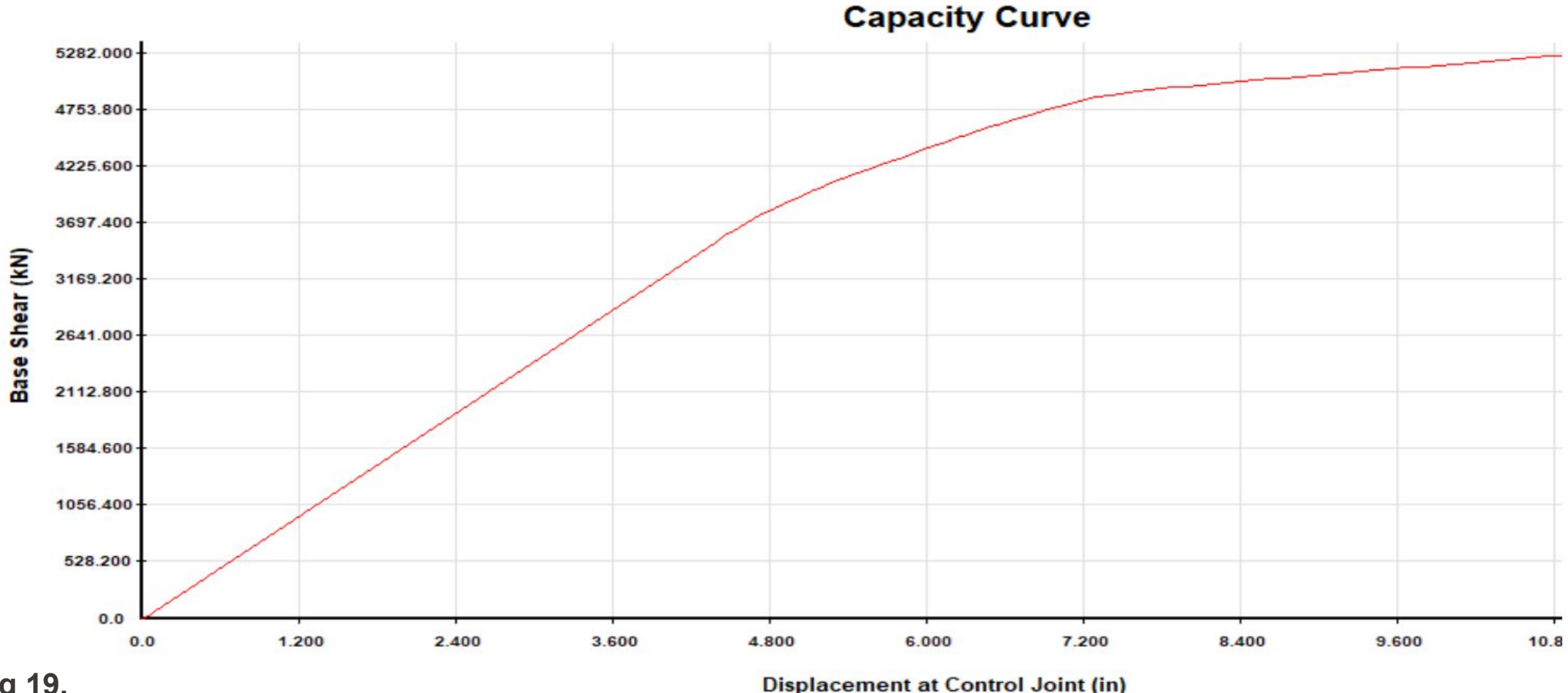


Fig 19.

CONCLUSION

- Nonlinear static analysis was used to successfully execute the notion of performance-based earthquake design by applying incremental lateral stresses to braced and non-braced steel frames. Using STAAD Pro. Advanced, the performance criteria provided by FEMA 356 can be successfully incorporated in the PBSD pushover analysis approach.
- Under incremental push loads, the maximum members of the moment frame reach the Collapse prevention level and eventually fail. This causes the entire steel frame to collapse during the earthquake. External steel bracings can be added to the structural system to boost the structure's shear capacity. However, bracing fails under progressive lateral loads.
- This causes structural members to fail during an earthquake since the maximum members are in the CP level. To avoid this, pushover analysis can be used to identify which members are failing following incremental lateral load and the position of bracing that prevents these members from failing.
- During an earthquake, this perfect bracing location saves the structure. It is determined that a properly braced steel frame boosts the structure's shear capacity and performs effectively, especially at the LS level. After incremental lateral loads, no member collapse is seen in this frame. Pushover analysis has been effectively used to investigate nonlinear structural behaviour under earthquake loading.

REFERENCES

- https://www.iitk.ac.in/nicee/wcee/article/13_1823.pdf
- <https://link.springer.com/article/10.1007/s40091-015-0080-y>
- <http://ignited.in/l/a/304875>
- https://www.iitk.ac.in/nicee/wcee/article/WCEE2012_1281.pdf
- http://www.i-ASEM.org/publication_conf/ASEM17/1.SM/XH3A.5.SM1130_4175F1.pdf
- <https://www.constrofacilitator.com/seismic-design-of-steel-moment-frames/>
- <https://www.mka.com/services/performance-based-seismic-design>
- <https://store.ctbuh.org/technical-guides/137-performance-based-seismic-design-for-tall-buildings.html>
- <https://onlinelibrary.wiley.com/doi/abs/10.1002/tal.637>
- <https://journals.sagepub.com/doi/abs/10.1193/1.1586128>
- <https://journals.sagepub.com/doi/abs/10.1193/1.4000046>
- <https://iopscience.iop.org/article/10.1088/1757-899X/910/1/012008/pdf>
- http://www.sqinstitute.in/activities/Civil/Day_6_1.pdf
- <https://www.iaset.us/IEEE-Civil>



Thank You